

DEVELOPMENT OF FLUOROTHERMOPLASTIC ELASTOMER
NANOCOMPOSITES BY DYNAMIC VULCANIZATION

By

WENBO XIN

A thesis completed in partial fulfillment of
the requirements for the degree of
MASTER OF SCIENCE IN MATERIALS SCIENCE

WASHINGTON STATE UNIVERSITY

Department of Mechanical and Materials Engineering

AUGUST 2010

To the Faculty of Washington State University,

The members of the Committee appointed to examine the thesis of WENBO XIN find it satisfactory and recommend that it be accepted.

Jinwen Zhang, Ph.D, Chair

Long Jiang, Ph.D

Katie Zhong, Ph.D

ACKNOWLEDGEMENTS

I would like to give thanks to the faculty and staff of WSU for your assistance and support during the last two years. Special thanks to committee chair and my advisor Dr. Jinwen Zhang, who has constantly provided constructive suggestions and support. And also I appreciate much for the advice and instructions directly from my committee member Dr. Long Jiang.

Meanwhile, I feel grateful for the assistance and dedication from another committee member, Dr. Katie Zhong. Actually, there are many people at Composite Materials and Engineering Center (CMEC) to thank, but I will try to give as much credit as possible. I will not be able to complete this research without the technical as well as administrative support from lab personnel such as Bob Duncan, Dr. Karl Englund, Dr. Vikram Yadama, Judy Edmister, Pat Smith and Janet Duncan. My thanks also go to all my colleagues at the lab who assisted me a lot on experiments. Finally, a special sign of appreciation goes out to my parents, brother and loving fiancé, who unconditionally give me emotional support on completing my graduate degree.

DEVELOPMENT OF FLUOROTHERMOPLASTIC ELASTOMER NANOCOMPOSITES BY DYNAMIC VULCANIZATION

Abstract

by Wenbo Xin, M.S.
Washington State University
August 2010

Chair: Jinwen Zhang

In this research, development of fluoropolymer nanocomposites was investigated. Fluoroelastomer (FKM) nanocomposites were prepared by melt mixing in a Haake rheometer and then the post cure and preparation of the test samples were carried out using compression molding. Effects of different nanofillers on fluoroelastomer vulcanization, mechanical and dynamic properties, and thermal stability were studied. It was found that the tested nanofillers had significantly different effects on the vulcanization of the fluoroelastomer, which in turn led to different mechanical, thermal dynamic, and thermal stability properties. In addition, a novel type of fluorothermoplastic elastomer (F-TPE) nanocomposites, were prepared by dynamic vulcanization method. The fluoroelastomer was partially vulcanized during blending and was cured further in a subsequent post cure process. Nanoclay, nano silica and expanded graphite were added to the blends and their effects on morphology, mechanical, dynamic, and thermal properties of the blends were studied. The nanofillers appeared to preferentially reside in the

elastomer phase of the blends. It was also found that all the nanofillers could increase the mechanical properties and storage modulus of the F-TPE blends. Thermal stability of the blends was influenced differently depending on the nanofiller type.

TABLE OF CONTENTS

ACKNOWLEDGEMENTS	iii
ABSTRACT.....	iv
TABLE OF CONTENTS.....	vii
LIST OF FIGURES	ixx
LIST OF TABLES.....	xii
CHAPTER 1—INTRODUCTION	1
1.1 Fluoropolymer and Fluoroelastomer	1
1.2 Thermoplastic Elastomer and Fluorothermoplastic Elastomer.....	3
1.3 Mechanisms of Reinforcement and Nanofillers	4
1.4 Crosslinking Mechanisms and Cure Kinetics.....	6
1.4.1 Curing of Natural Rubbers.....	6
1.4.2 Curing of Fluoroelastomers.....	8
1.5 Dynamic Vulcanization and Thermo Haake Rheometer	13
1.6 Current Research and Objectives.....	16
1.6.1 Current Research.....	16
1.6.2 Objectives.....	17
1.7 Reference.....	19
CHAPTER 2—CUREING KINETICS AND PROPERTIES OF FLUROELASTOMER NANOCOMPOSITES	22
2.1 Abstract	22
2.2 Introduction.....	23

2.3 Experimental	26
2.3.1 Materials	26
2.3.2 Silica and Graphite Treatments.....	27
2.3.3 Study of Vulcanization by Torque Rheometry and DSC.....	28
2.3.4 Other Characterizations	30
2.4 Results and Discussion	34
2.4.1 Factors Influencing Cure Behaviors of Fluoroelastomer Nanocomposites	34
2.4.2 Vulcanization Kinetics during Post Cure.....	37
2.4.3 Dynamic Mechanical Properties.....	40
2.4.4 Tensile Properties.....	45
2.4.5 Thermal Stability	47
2.4.6 Morphology of FC 2260 Nanocomposites.....	51
2.5 Conclusions.....	58
2.6 Reference	59
CHAPTER 3— PREPARATIONS AND PROPERTIES OF FLUOROTHERMOPLASTIC ELASTOMER NANOCOMPOSITES PROCESSED THROUGH DYNAMIC VULCANIZATION.....	63
3.1 Abstract	63
3.2 Introduction.....	64
3.3 Experimental	67
3.3.1 Materials	67
3.3.2 Preparations.....	68

3.3.3 Characterizations.....	69
3.4 Results and Discussion	70
3.4.1 Dynamic Mechanical Properties	70
3.4.2 Tensile Properties.....	75
3.4.3 Thermal Stability	79
3.4.4 Dispersion and Morphology	81
3.5 Conclusions.....	88
3.6 Reference	89
CHAPTER 4—CONCLUSIONS AND FUTURE WORK.....	91
4.1 Conclusions.....	91
4.2 Future Work.....	92
APPENDIX—DATA SHEET OF FC 2260 AND FEP 6322.....	94

LIST OF FIGURES

Figure 1.1 Polymerization of PTFE	1
Figure 1.2 Schematic showing classifications of polymer/clay nanocomposites	5
Figure 1.3 Illustration of the function of silane coupling agent.....	6
Figure 1.4 Probable reactions from peroxide decompositions and proposed crosslinking mechanism.....	11
Figure 1.5 Structure of triallyl isocyanurate (TAIC).....	12
Figure 1.6 Picture of a Haake Toque Rheometer.....	15
Figure 2.1 Tensile testing set-up with the tensile strain measured by a laser extensometer	33
Figure 2.2 Mixing torque-time curves of FKM formulations.....	36
Figure 2.3 Calculation of activation energy from non-isothermal DSC data based on Kissinger equation.....	38
Figure 2.4 Storage modulus spectra for different formulations of FKM Nanocomposites.....	43
Figure 2.5 Damping peaks of different formulations of FKM nanocomposites.....	44
Figure 2.6 Tensile properties of different FKM nanocomposites comprising different types of nanofillers.....	46
Figure 2.7 Representative TGA curves showing the effects of fillers on thermal stability of FKM nanocomposites.....	50
Figure 2.8 TGA curves showing weight loss of the different types of nanofillers.....	51

Figure 2.9 SEM images of treated silica and treated graphite compared to untreated silica and graphite flake.....	53
Figure 2.10 SEM images of FC 2260/UT-SiO ₂ , FC 2260/T- SiO ₂ and FC 2260/T-G formulations.....	57
Figure 3.1 Storage modulus and tanδ curves of neat F-TPE and F-TPE nanocomposites comprising 2% of different nanofillers.....	72
Figure 3.2 Comparison of the storage modulus and tanδ of F-TPE nanocomposites comprising 4% different nanofillers.....	74
Figure 3.3 Tensile properties of F-TPE nanocomposites comprising 2% and 4% of different nanofillers	77
Figure 3.4 Thermal stability of neat F-TPE and F-TPE nanocomposites.....	81
Figure 3.5 SEM images of neat F-TPE, and F-TPE/2% UT-SiO ₂ and F-TPE/2% T- SiO ₂ formulations.....	85
Figure 3.6 Cryo-sliced surfaces of neat F-TPE, and F-TPE/2% UT-SiO ₂ and F-TPE/2% T-SiO ₂ and F-TPE/2% T-G.....	86
Figure 3.7 SEM images of neat F-TPE and F-TPE/2% T- SiO ₂ and TEM image of F-TPE/2% T- SiO ₂ formulation.....	87

LIST OF TABLES

Table 2.1 Formulations of fluoroelastomer nanocomposites.....	32
Table 2.2 Thermal characteristics of fluoroelastomer nanocomposites.....	43
Table 2.3 Tensile properties of FC 2260 nanocomposites.....	47
Table 3.1 Formulations of neat F-TPE and F-TPE nanocomposites.....	69
Table 3.2 Thermal analysis results of neat F-TPE nanocomposites and F-TPE nanocomposites.....	75

CHAPTER 1

INTRODUCTION

1.1 Fluoropolymer and Fluoroelastomer

In 1930s, Dr. Roy J. Plunkett discovered a new type of polymer—fluoropolymer, when he was polymerizing tetrafluoroethylene to form polytetrafluoroethylene (PTFE). This new material was registered as Teflon® in 1944 and since then many forms of PTFE and copolymers of fluorinated polymers have been developed and commercialized. Generally, a fluoropolymer is defined as a polymer consisting of carbon (C) and fluorine (F) (Ebnesajjad and Khaladkar 2005). Fluoropolymer are usually classified as two main categories: fluoroelastomers, some of which are curable and fluorothermoplastics which possess excellent processability. Due to the high stability of fluorine-carbon bond, fluoropolymers have excellent chemical and heat resistance, low friction coefficient, and low permeability. Figure 1.1 showed the polymerization process of PTFE.

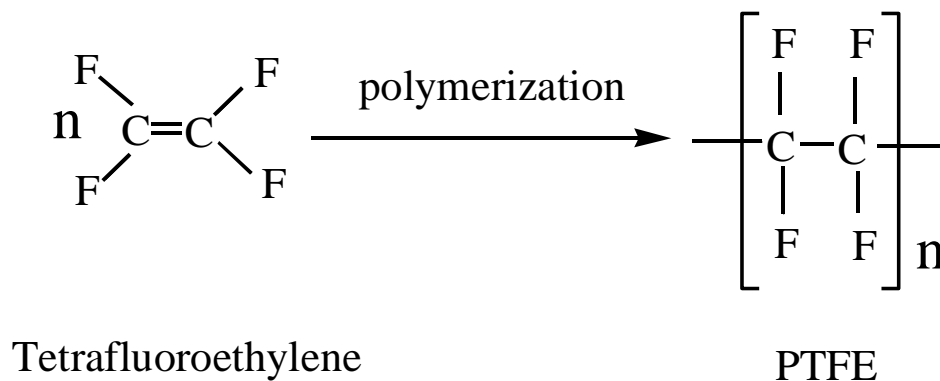


Figure 1.1 Polymerization of PTFE

There are two general types of rubbers or elastomers, i.e., crosslinked elastomer and thermoplastic elastomer (TPE). Most of the commonly used rubbers are crosslinked ones with their chains chemically bonded during the curing process. Once formed, this type of rubber cannot be reprocessed, softened, melted or reshaped by following reheating. Thermoplastic elastomers, on the other hand, are rubbers which act in a way similar to crosslinked materials but are copolymers or physical mix of thermoplastics and rubbers with both thermoplastic and elastomeric properties. These elastomers are usually hydrocarbon-based polymers mainly consisting of carbon and hydrogen atoms.

Fluoroelastomers, as a special kind of elastomers, are widely used in many industrial applications due to their excellent heat, oil and solvent resistances (Kader and Nah 2004). Regarding the structure of monomer, main families of fluoroelastomers include dipolymer of vinylidene fluoride (VDF)/ hexafluoropropylene (HFP), terpolymer of vinylidene fluoride (VDF)/hexafluoropropylene (HFP)/tetrafluoroethylene (TFE), and peroxide-vulcanizable polymers which are similar to terpolymers (Jagels, 2005). Fluoroelastomers meet rigorous performance requirements in harsh environments, enhancing reliability, safety, and environmental friendliness. Fluoroelastomers are growing as products of choice for critical components such as O-rings, hoses, and seals in hostile fluid and temperature conditions. These elastomers are mostly compounded with inorganic fillers such as carbon black, silica, clay, etc. to enhance the mechanical properties, to change the electrical conductivity, to improve the barrier properties or to increase the resistance to fire and ignition. However, a minimum of 20 wt% of the filler content is always required for a critical property enhancement, which may lead to many problems in processing and curing, such as reducing the processability of the elastomer

compounds, causing the end products to weigh significantly more than the neat rubber. In the last few decades, the concept of nanocomposites has shown great potential to alleviate the problem of high loading of particulate fillers in the elastomeric matrix.

Nanocomposites give manifold increase in useful properties by dispersing small amount of nano scale filler such as layered silicate (clay) in the polymer matrix. However, to achieve good dispersion, the layers of the silicate should undergo intercalation and exfoliation (delamination) in the polymer matrix.

1.2 Thermoplastic Elastomer and Fluorothermoplastic Elastomer

Thermoplastic elastomers (TPE) have been attracted much attentions since 1950s, when they became a commercial reality. TPE, sometimes referred as thermoplastic rubbers, are a class of copolymers or a physical mix of a plastic and a elastomer which consist of materials with both thermoplastic and elastomeric properties. In this study, fluorothermoplastic elastomer (F-TPE) is defined as a specific TPE which contains fluorothermoplastic and fluoroelastomer. Generally, these types of materials show the following advantages: (1) both advantages typical of rubbery materials and plastic materials, (2) processable and recyclable like thermoplastic, (3) great improvement of properties achieved by the addition of small amount of nanofillers. While the advantages of F-TPE lead to extensive applications, the limitations are also obvious: high cost of raw materials, insufficient mechanical and thermal stability which might not be enough for certain uses. To overcome these disadvantages, different nanofillers can be used to improve the F-TPE's properties. Detailed information, experiments and results will be introduced in the following chapters.

1.3 Mechanisms of Reinforcement and Nanofillers

Fillers have been used in the formulation of polymer composites since early years of the polymer industry. It has been found that fillers can not only function as cost-reducing materials, but also act as reinforcing materials in polymer composites and rubbers to improve their tensile strength (Ten et al. 2010), modulus (Schmidt and Giannelis 2010), tear resistance (Peng et al. 2007), and abrasion resistance (Avella, et al. 2001). Therefore, very few rubber compounds are prepared without the addition of substantial quantities of fillers. The performance of fillers in the rubber matrix is controlled by its characteristics, such as particle size, concentration, shape, structure of particle agglomerates and degree of interactions with the matrix (Jiang, et al. 2007). The degree of bonding between filler particles and rubber matrix is a key factor in determining the reinforcing effects of the particles. The two most widely used reinforcing fillers in the rubber industry are carbon black and clay. For example, Heinrich and Vilgis (1993) reported that carbon black showed an influence on crosslinking of polybutadiene and significantly increased its shear modulus. Also, fully exfoliated clay in epoxy matrix improved the storage modulus apparently (Park and Jana 2003). In order to achieve maximum reinforcement, the loading of these fillers should be appreciably high, which often creates processing problems. However, if the size of the fillers is in nano scale, the introduction of these nano-sized (e.g. nanoclay, nanosilica, etc.) fillers can result in polymer nanocomposites exhibiting multifunctional, high-performance characteristics beyond what traditional filled polymeric materials possess. Although layered silicate nanocomposites have been prepared and characterized for many thermoplastic and thermosetting polymers, much

less attention has been paid to rubber/clay nanocomposites, especially some specialty elastomers, such as fluoroelastomers.

Depending on compounding methods and the interfacial interactions between nanoclay and elastomer matrix, three main types of morphologies of elastomer-clay composites can be produced as shown in Figure 1.2 (Koo 2006):

- (a) Unintercalated: the regular layered structure (stack) of originally modified nanoclay is not disrupted, and nanoclay is dispersed like a regular particulate filler.
- (b) Intercalated: this state is formed by the insertion of rubber chains between the nanoclay layers, the ordered structure of layers is retained..
- (c) Exfoliated: In this state, individual layers of the nanoclay are completely delaminated and dispersed in the rubber matrix. The ordered structure of the layered nanoclay is lost.

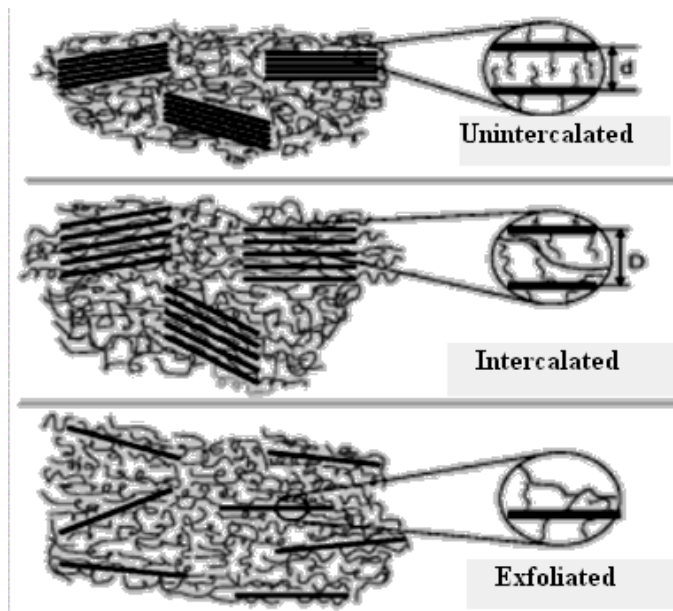


Figure 1.2 Schematic showing classifications of polymer/clay nanocomposites (Koo 2006).

Besides nanoclay, nanosilica and graphite are two other important reinforcing nanofillers. The surface of the nanosilica is often treated to increase its compatibility with the polymer matrix and hence to improve mechanical properties of the nanocomposites. There are several ways to modify silica nano particles and graphite. For example, as shown in Figure 1.3, the silica nano particles (Xu and Chung 1999) and the matrix can be coupled with silane, where the functional group (in this case, the amino group) attaches to an organic resin (matrix) while the functional groups (X) attach to inorganic material (silica) to achieve a “coupling” effect.

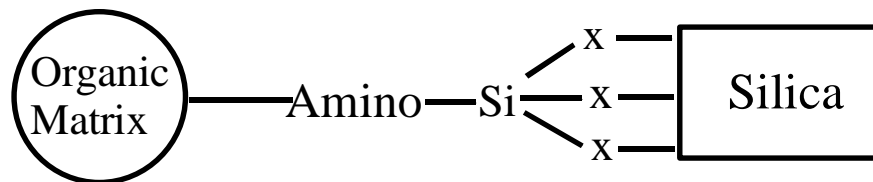


Figure 1.3 Illustration of the function of silane coupling agent.

1.4 Crosslinking Mechanisms and Cure Kinetics

1.4.1 Curing of Natural Rubbers

Peroxide and sulfur are the most widely used crosslinking agents for uncured natural elastomers. The chemical reaction consisting in the addition of sulfur to the double bonds of the rubber molecules are always involved in the vulcanization of rubber with sulfur, which constantly forms the three dimensional networks (Lewis, et al. 1937). For peroxide curing, the free radical produced by peroxide is the driving force for peroxide crosslinking, which is much faster than sulfur cure. Free radicals are atoms or molecular

fragments with unpaired electrons, which are in unstable state and tend to react with other materials to make the electron to pair with another. The process of rubber peroxide crosslinking consists of three basic steps as follows (Moore 2005).

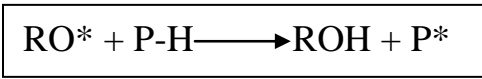
(a) Homolytic cleavage

When a peroxide is heated to above its decomposition temperature, the oxygen-oxygen bond ruptures. The resulting molecular fragments are called free radicals, which are reactive species with high energy.



(b) Hydrogen abstraction

Those radicals that are generated from the peroxide decomposition are reactive to hydrogen atoms in the polymer chains. Hydrogen abstraction is a process that the radical removes a hydrogen atom from another nearby atom, through which radicals are transferred from the peroxide molecular fragments to the rubber backbone.



(c) Radical coupling

Rubber radicals are highly reactive species and when the two of these radicals come in contact, the unpaired electrons will couple and form a covalent bond or crosslink between the rubber chains.



1.4.2 Curing of Fluoroelastomers

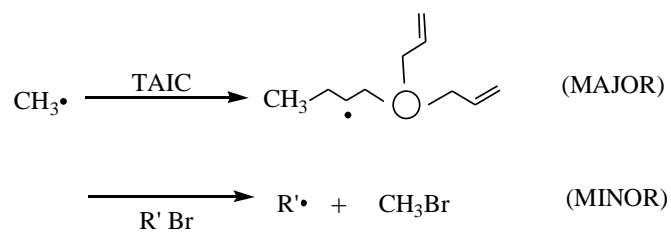
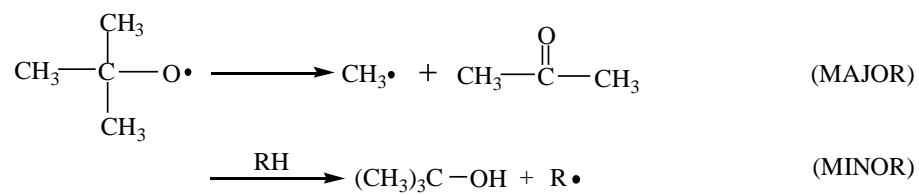
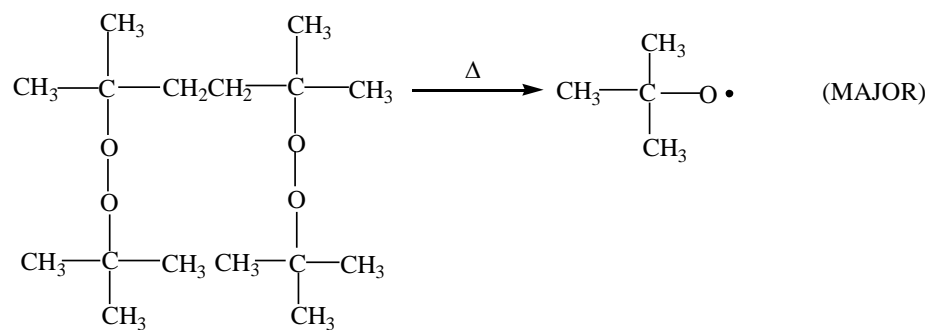
There are usually three types of curing agents for fluoroelastomer vulcanization, peroxide, diamine and bisphenol, with various curing mechanisms, respectively.

Different from peroxide curing with free radicals, diamine curing is based on the addition of diamine to the polymer chain after the VDP type fluoroelastomer is subjected to dehydrofluorination in the presence of basic media which can extract hydrofluoride from the elastomer (Salamone 1999). Another curing agent for fluoroelastomer is bisphenol, and the crosslinking mechanism mainly includes three steps, i.e. dehydrofluorination by hydroxide ions, substitution of fluorine atoms by bisphenol and elimination of HF (Taguet, et al. 2005).

Fluoroelastomers cured with peroxides, or free radicals, exhibit improved resistance to steam, hot water, and aqueous acids over those cured with bisphenols. Peroxide-cured compounds generally do not contain much inorganic bases, so they are less susceptible to attack by aqueous fluids. On the other hand, the curing of fluoroelastomers using peroxide requires crosslinking agents (“radical traps”), and the resulting compounds give lower thermal stability than that cured with bisphenols. For peroxide curing, fluoroelastomers must contain sites reactive toward free radicals, usually bromine or iodine introduced within chains by incorporation of cure-site monomers or at chain ends by chain-transfer agents. In the late 1970s, DuPont offered the first commercial peroxide-curable fluoroelastomers which had a bromine-containing cure-site monomers (i.e., 4-

bromo- 3,3,4,4-tetrafluorobutene (BTFB), and the total bromine comprised of 0.5 – 0.9 wt% of the fluoroelastomer. Reaction conditions in the continuous emulsion polymerization process can be adjusted to minimize unwanted transfer to incorporated bromine-containing units, thus avoiding excessive long-chain branching. Such transfer and branching reactions are more difficult to minimize in semi-batch processes, since the entire polymer formed remains in the reactor exposed to free radical activity until the end of the batch polymerization.

Figure 1.4 shows the probable cure reactions resulting from initiator decomposition in a typical peroxide compound (Moore 2005). Most of the primary *t*-butoxy radicals undergo β -scission to acetone and methyl radicals. A major fraction of the methyl radicals add to the allyl functionality of the triallyl isocyanurate (TAIC) coagent to form radical adducts. Only a minor fraction of methyl radicals is involved in transfer reactions with fluoroalkyl bromide sites on polymer chains to form methyl bromide and polymeric radicals. If the radical trap concentration is reduced considerably, the amount of methyl bromide increases by up to a factor of two, still relatively low versus the total amount of methyl radicals produced.



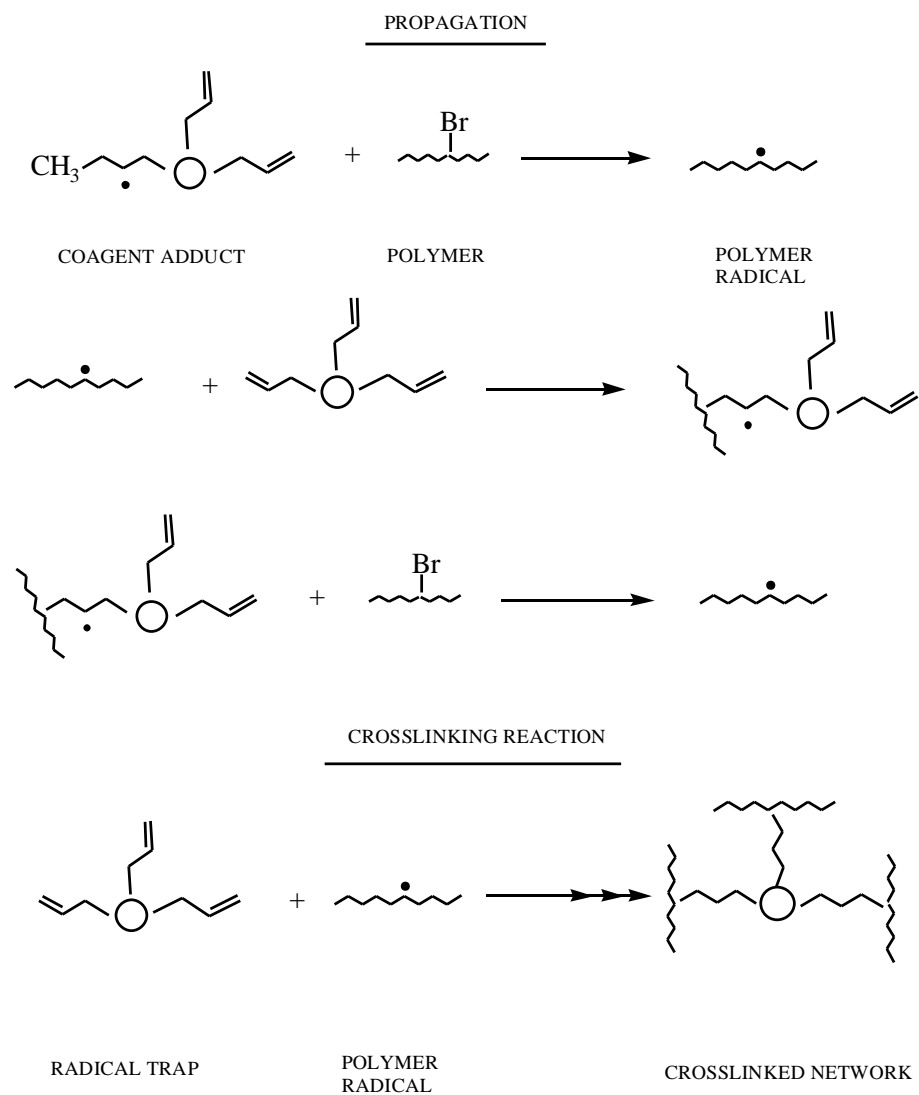


Figure 1.4 Probable reactions from peroxide decompositions and proposed crosslinking mechanism (Moore 2005).

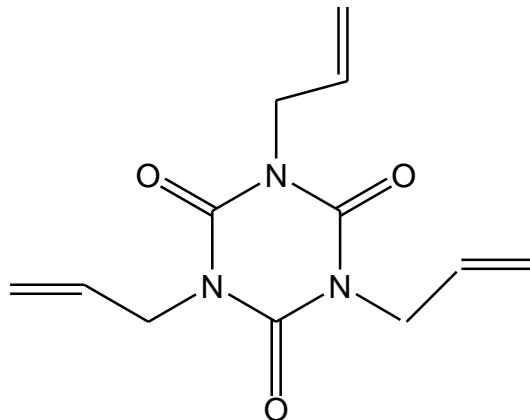


Figure 1.5 Structure of triallyl isocyanurate (TAIC).

In a study of peroxide curing of bromine-containing fluoroelastomers, DuPont researchers obtained satisfactory cures with aliphatic peroxides 2,5-dimethyl-2,5-di-*t*-butylperoxyhexane, and 2,5-dimethyl-2,5-di-*t*-butylperoxyhex-3-yne, available from Atochem as Luperc 101XL and 130XL (45% active ingredient on inert support) (Moore 2005). These peroxides have a half life of 0.8 and 3.4 minutes at 177 °C, respectively. Lower molecular weight aliphatic peroxides such as di-*t*-butylperoxide were found to be active, but too volatile, being partially lost during compound mixing. Peroxides containing aromatic substituent (e.g., dicumyl peroxide), gave variable results, probably because of excessive acid-catalyzed decomposition in the fluoroelastomer matrix. Of the radical traps tested, the most effective crosslinker is TAIC, as judged by cure state and compression set of vulcanizates. Other effective crosslinkers contain unhindered allyl or vinyl groups attached to N, O, or Si; all are electron-rich groups. Electron-poor traps are effective in hydrocarbon elastomers, such as *m*-phenylene-bis-maleimide, are ineffective

in fluoroelastomers (Moore 2005). Structures of the effective radical traps TAIC, are shown in Figure 1.5.

Generally, there are many ways to calculate curing kinetics of rubber crosslinking process, such as Horie model (Cole 1991). The widespread method is using the activation energy of the cure reaction determined by both Kissinger's and Ozawa's methods (Wang and Lin 2000) for accuracy of results. Based on Kissinger's theory, the activation energy can be obtained from the peak temperatures at different heating rates (Liu, et al. 2009). The equation is expressed as:

$$-\ln(q/T_p^2) = E_a/RT_p - \ln(AR/E_a)$$

where q is the heating rate, T_p is the exothermic peak temperature, E_a is the activation energy, R is the gas constant and A is the pre-exponential factor. A plot of $-\ln(q/T_p^2)$ versus E_a/RT_p should be linear and the apparent activation energy can be obtained from the slope of the straight line.

1.5 Dynamic Vulcanization and Thermo Haake Rheometer

As mentioned above, elastomer/thermoplastic blends have become technologically and commercially viable as thermoplastic elastomers in recent years. They have many properties of elastomers, yet they are processable like thermoplastic. They do not need to be vulcanized during fabrication into end-use parts. Thus, they offer a substantial economics, design, and processing advantage regarding the fabrication of the finished parts. For many end uses, the ideal elastomer/plastic blend comprises finely divided

elastomer particles dispersed in a relatively small amount of plastic. The elastomer particles should be crosslinked to promote elasticity. This favorable morphology should remain during the fabrication of the material into parts, and during end use. The usual methods for preparing elastomer/plastic blends by melt mixing, solution blending, or latex mixing are not sufficient since elastomer phase cannot be cured during processing.

The best way to produce thermoplastic elastomeric composites comprising vulcanized elastomer particles in melt-processable matrices is by a method called dynamic vulcanization (Holden, et al. 2004). It is the process of vulcanizing an elastomer during its melt-mixing with a non-vulcanizing thermoplastic polymer. Small elastomer droplets are vulcanized to give a particulate vulcanized elastomer phase of stable domain morphology during melt processing. The main purpose of the dynamic vulcanization of elastomer-plastic blends is to produce compositions which have the improvement in permanent set, ultimate mechanical properties, fatigue resistance, hot oil resistance, high-temperature utility, melt strength, and thermoplastic fabricating ability.

In this study, Mixing of ingredients of the formulated composites and dynamic vulcanization of the elastomer was performed using a Haake torque rheometer. This device is shown in Figure 1.6. The Haake torque rheometer is an innovative torque rheometer platform designed to optimize process engineering applications. Data for melt characteristics, viscosity under shear load and the effectiveness of additives, heat and shear stability are readily attainable with this system.

A typical mixer test is run at a defined speed (shear rate) versus time, and the material's response is recorded as torque. The mixing chamber is temperature-controlled precisely by independent heating and cooling zones, but due to the frictional heat in the

mixing bowl, a change in the material's melt temperature is observed and recorded as measuring signal. This "Rheogram" (torque, melt temperature vs. time at constant speed) is characteristic for different materials or blends. For experiment in the lab, haake toque rheometer has two main advantages. First, it is economic since less amount of materials can be utilized compared with extrusion. Second, the relationship of toque versus time from haake processing presents curing state of raw materials, from which curing behavior of elastomer might be obtained.



Figure 1.6 Picture of a Haake Toque Rheometer

1.6 Current Research and Objectives

1.6.1 Current Research

In the current research, silica and graphite, as attractive types of nanofillers for polymer composites, has gathered much research interest. Storage modulus of polyvinyl acetate (PVAc) was found to increase after the incorporation of nanosilica (Sternstein and Zhu 2002). With the presence of untreated silica nanopowder in PP matrix, tensile strength, Young's modulus as well as toughness of the polymer nanocomposites increased apparently (Rong, et al. 2001). Furthermore, thermal degradation temperature of polyimide/silica nanocomposites was enhanced significantly from 561 °C of the neat polymer to 581, 588, 600 °C by adding 10%, 20%, 30% silica, respectively (Chen, et al. 2004). Graphite is usually treated by oxidation and thermal expansion to get favorable monolayer structures which is named as graphene (Geim and Novoselov 2007). Ramanathan et al. reported that only 0.05 wt% treated graphite in polymethyl methacrylate (PMMA) offered an improvement of nearly 30 °C in glass transition temperature of the polymer (Ramanathan, et al. 2008).

For fluoropolymer nanocomposites study, nanoclays have been used as reinforcing fillers most frequently. Nanoclay was found to affect vulcanization kinetics of a fluoroelastomer. It could effectively reduce the energy requirement for the curing process of the fluoroelastomer (Kader and Nah 2004) and increase the thermal degradation temperature of the fluoroelastomer in both nitrogen and oxygen atmospheres (Kader, et al. 2006). Meanwhile, M. Maiti, et al., pointed out the concentration of nanoclay in fluoroelastomer influenced dynamic mechanical properties of the composites and 20 wt% nanofiller provided the optimized storage modulus (Maiti and Bhowmick 2006).

There are also many studies on thermoplastic elastomer. It has been shown that many TPEs, e.g., diene rubber/polyolefin blend-based thermoplastic elastomer (Fischer 1985), butyl rubber/polypropylene blend-based thermoplastic elastomer (Liao, et al. 1994), and acrylic rubber/poly(vinylidene fluoride) blend-based thermoplastic elastomer (Li, et al. 2006), show higher mechanical properties, such as tensile strength, tensile modulus and storage modulus, through dynamic vulcanization.

1.6.2 Objectives

Nanofillers such as nanoclays, silica nanoparticles, and functionalized graphene sheets have been reported to improve mechanical and thermal properties of the polymer matrixes, which are mainly traditional non-fluoropolymers such as PMMA, PU, and PVAc, etc. To the best of our knowledge, little research has been done on the effects of nanofillers (e.g., treated silica and functionalized graphene) on mechanical and physical properties of the high-performance fluoroelastomers. This is especially true for fluoropolymer/graphene nanocomposites. No studies and results can be found on this type of nanocomposites in the open literature.

On the other hand, though many studies of TPEs have been carried out, the influence of nanofillers on mechanical and thermal properties of high performance TPE systems, i.e., fluorothermoplastic elastomer (F-TPE), still needs to be further investigated. Further, the effects of nanofillers on dynamic vulcanization of F-TPE and on morphology of the resulting F-TPE nanocomposites also deserve an in-depth investigation.

In this study, different types of nanofillers were employed to reinforce the fluoroelastomer. Their effects of the nanofillers on curing kinetics, mechanical and

dynamic properties, and thermal stability of the fluoroelastomer were investigated.

Moreover, the effects of nanofillers on F-TPE blends were also systematically studied.

The objectives of this study included:

(1) developing fluoroelastomer nanocomposites and F-TPE nanocomposites with improved properties;

(2) understanding the effects of different nanofillers on curing behavior of the fluoroelastomer and mechanical and thermal properties of fluoroelastomer and F-TPE and;

(3) understanding the morphology and properties of the F-TPE nanocomposites.

1.7 Reference

- Avella, M., M. E Errico, and E. Martuscelli. 2001. "Novel PMMA/CaCO₃ nanocomposites abrasion resistant prepared by an in situ polymerization process." *Nano Letters* 1:213–217.
- Chen, B. K, T. M Chiu, and S. Y Tsay. 2004. "Synthesis and characterization of polyimide/silica hybrid nanocomposites." *Journal of Applied Polymer Science* 94:382–393.
- Cole, K. C. 1991. "A new approach to modeling the cure kinetics of epoxy/amine thermosetting resins. 1. Mathematical development." *Macromolecules* 24:3093–3097.
- Ebnesajjad, S., and P. R Khaladkar. 2005. *Fluoropolymers applications in chemical processing industries: the definitive user's guide and databook*. William Andrew Inc.
- Fischer, W. K. 1985. *Dynamically partially cured thermoplastic blend of monoolefin copolymer rubber and polyolefin plastic*. Google Patents.
- Geim, A. K., and K. S. Novoselov. 2007. "The rise of graphene." *Nature materials* 6:183–191.
- Heinrich, G., and T. A. Vilgis. 1993. "Contribution of entanglements to the mechanical properties of carbon black-filled polymer networks." *Macromolecules* 26:1109–1119.
- Holden, G., H. R Kricheldorf, and R. P Quirk. 2004. *Thermoplastic elastomers*. Hanser Verlag.
- Jiang, L., J. Zhang, and M. P Wolcott. 2007. "Comparison of polylactide/nano-sized calcium carbonate and polylactide/montmorillonite composites: Reinforcing effects and toughening mechanisms." *Polymer* 48:7632–7644.
- Kader, M. A, M. Y Lyu, and C. Nah. 2006. "A study on melt processing and thermal properties of fluoroelastomer nanocomposites." *Composites Science and Technology* 66:1431–1443.
- Kader, M. A, and C. Nah. 2004. "Influence of clay on the vulcanization kinetics of fluoroelastomer nanocomposites." *Polymer* 45:2237–2247.
- Koo, J. H. 2006. *Polymer nanocomposites: processing, characterization, and applications*. McGraw-Hill Professional.

- Lewis, W. K., L. Squires, and R. D Nutting. 1937. "Mechanism of Rubber Vulcanization with Sulfur." *Industrial & Engineering Chemistry* 29:1135–1144.
- Li, Y. et al. 2006. "A novel thermoplastic elastomer by reaction-induced phase decomposition from a miscible polymer blend." *Macromolecules* 39:4195–4201.
- Liao, F. S, A. C Su, and T. C.J Hsu. 1994. "Damping behaviour of dynamically cured butyl rubber/polypropylene blends." *Polymer* 35:2579–2586.
- Liu, X., W. Xin, and J. Zhang. 2009. "Rosin-derived imide-diacids as epoxy curing agents for enhanced performance." *Bioresource Technology*.
- Maiti, M., and A. K Bhowmick. 2006. "Effect of solution concentration on the properties of nanocomposites." *Journal of Applied Polymer Science* 101:2407–2411.
- Moore, A. L. 2005. *Fluoroelastomers handbook: the definitive user's guide and databook*. William Andrew Publishing.
- Park, J. H, and S. C Jana. 2003. "Mechanism of Exfoliation of Nanoclay Particles in Epoxy- Clay Nanocomposites." *Macromolecules* 36:2758–2768.
- Peng, Z., L. X Kong, S. D Li, Y. Chen, and M. F Huang. 2007. "Self-assembled natural rubber/silica nanocomposites: Its preparation and characterization." *Composites Science and Technology* 67:3130–3139.
- Ramanathan, T. et al. 2008. "Functionalized graphene sheets for polymer nanocomposites." *Nature Nanotechnology* 3:327–331.
- Rong, M. Z et al. 2001. "Structure-property relationships of irradiation grafted nano-inorganic particle filled polypropylene composites." *Polymer* 42:167–183.
- Salamone, J. C. 1999. *Concise polymeric materials encyclopedia*. CRC.
- Schmidt, D. F, and E. P Giannelis, 2010. "Silicate Dispersion and Mechanical Reinforcement in Polysiloxane/Layered Silicate Nanocomposites." *Chemistry of Materials* 2132.
- Sternstein, S. S., and A. J Zhu. 2002. "Reinforcement mechanism of nanofilled polymer melts as elucidated by nonlinear viscoelastic behavior." *Macromolecules* 35:7262–7273.
- Steve Jagels, 2005. "A Guide to Fluoroelastomers". Solvay Solexis, Inc.
- Taguet, A., B. Ameduri, and B. Boutevin. 2005. "Crosslinking of Vinylidene Fluoride-Containing Fluoropolymers." *Crosslinking in Materials Science* 127–211.

Ten, E., J. Turtle, D. Bahr, L. Jiang, and M. Wolcott. 2010. "Thermal and Mechanical Properties of Poly (3-hydroxybutyrate-co-3-hydroxyvalerate)/cellulose nanowhiskers Composites." *Polymer*.

Wang, C. S., and C. H Lin. 2000. "Novel phosphorus-containing epoxy resins. Part II: curing kinetics." *Polymer* 41:8579–8586.

Xu, Y., and D. D. L. Chung. 1999. "Carbon fiber reinforced cement improved by using silane-treated carbon fibers." *Cement and Concrete Research* 29:773–776.

CHAPTER 2

CURING KINETICS AND PROPERTIES OF FLUOROELASTOMER NANOCOMPOSITES

2.1 Abstract

Fluoroelastomer (FKM) nanocomposites were prepared by melt mixing in a Haake rheometer and then the post cure and preparation of the test samples were carried out using compression molding. Five types of different nanofillers, i.e., surfactant treated clay (S-clay), fluoro-surfactant treated clay (FS-clay), untreated silica (U-SiO₂), treated silica (T-SiO₂), treated graphite (T-G) were used. Effects of these nanofillers on fluoroelastomer vulcanization, mechanical and dynamic properties, and thermal stability were studied. Vulcanization behavior of the fluoroelastomer was characterized by mixing torque and non-isothermal vulcanization kinetics. Tensile tests were performed on the compressed composite sheets to evaluate their mechanical properties. Glass transition and viscoelastic behavior of the nanocomposites were characterized by dynamic mechanical analysis (DMA). Thermal stability of the nanocomposites was evaluated by thermal gravimetric analysis (TGA). It was found that the tested nanofillers had significantly different effects on the vulcanization of the fluoroelastomer, which in turn led to different mechanical, thermal dynamic, and thermal stability properties.

2.2 Introduction

Polymer nanocomposites have attracted intensive research interest from both academia and industry in the last several decades. This is due to the significant increase in polymer mechanical, thermal, and barrier properties after the incorporation of a small amount of nanofillers such as nanoclay, silica nanoparticle, and functionalized graphene et al. Many studies have been performed on different thermoplastic polymer-nanofiller systems including polylactide (PLA)-clay (Jiang, et al. 2007), polypropylene (PP)-silicate (Gianelli, et al. 2005), polystyrene (PS)-clay (Zeng and Lee 2001), and polyamide (PA)-layered silica (Kim, et al. 2001), on thermoset polymer-nanofiller systems such as epoxy-cellulose nanofiber (Shimazaki, et al. 2007), and on rubber-nanofiller systems such as natural rubber (NR)-clay (Joly, et al. 2002), nitrile rubber (NBR)-clay (Kim, et. al. 2003), and ethylene-propylene rubber (EPM, EPDM)-single-walled carbon nanotubes (Valentini, et al. 2003).

Silica nanoparticle has been extensively investigated for its potential to improve various properties of polymers. Storage modulus of polyvinyl acetate (PVAc) was found to increase after the incorporation of nanosilica (Sternstein and Zhu 2002). Since one of the critical motivations for the addition of the silica particles is to enhance the mechanical properties, the improvement of mechanical properties of polymer nanocomposites is most concerned. (Zou, et al.2008). With the presence of untreated silica nanoparticle in PP matrix, tensile strength, Young's modulus and toughness of the polymer nanocomposites increased apparently (Rong, et al. 2001). Other mechanical properties such as impact strength and elongation at break of the polyamide 6/ modified silica nanocomposites prepared by in situ polymerization showed a tendency to increase and then decrease with

increasing silica content with the maximum values at 5% silica content (Yang, et al. 1998). Not only that, the thermal degradation temperature of polyimide/ silica nanocomposites was enhanced significantly from 561 °C to 581, 588, 600 °C by increasing the silica content to 10%, 20%, and 30%, respectively (Chen, et al. 2004).

Graphene, a new type of nanofiller for polymer composites, has started to gather research interest in the last few years. Graphene is a flat monolayer of carbon atoms tightly packed into a two dimensional honeycomb lattice (Geim and Novoselov 2007) and exhibits excellent mechanical properties (Dikin, et al. 2007; Lee, et al. 2008) and super thermal stability (Balandin et al. 2008). Currently, there are several methods available to prepare graphene including chemical vapor deposition (Novoselov, et al. 2004), direct sonication (Lotya, et al. 2009) and thermal expansion of graphite (Schniepp, et al. 2006). Thermally treated graphite (graphene) have shown wrinkled topology at the nanoscale and likely resulted in mechanical interlocking with the polymer chains (McAllister, et al. 2007). Ramanathan et al. (2008) reported that 0.05% treated graphite in polymethyl methacrylate (PMMA) offered a nearly 30 °C increase in glass transition temperature of the polymer (Ramanathan, et al. 2008). Furthermore, the addition of only 0.6% functionalized graphene (treated in a mixture of concentrated nitric acid, concentrated sulfuric acid and distilled water) to polyvinyl alcohol (PVA) resulted in an 35 and 45% increase in sample elastic modulus and hardness, respectively (Das, et al. 2009).

Recently, increasing attention has been paid to polymer-nanocomposites based on specialty polymers such as fluoropolymer. Fluoropolymer is the polymer comprising significant amount of fluorinated repetition units. It has excellent chemical and heat

resistance, low friction coefficient, and low permeability. Fluoropolymer can be categorized into two large groups, i.e. fluorothermoplastics and fluoroelastomers. Fluorothermoplastics can be melted repeatedly and processed by conventional melt-processing techniques such as extrusion and injection molding. Fluoroelastomers are elastomeric polymers which are crosslinked for high performance and cannot be melt processed again after crosslinking. It has been shown that fluoroelastomer/clay nanocomposites can achieve significant improvement in mechanical and thermal properties such as stiffness, modulus, strength, and heat distortion temperature with small contents of nanoclay (Maiti, et al. 2008). This type of materials is in great demand in critical industrial and aerospace applications.

To the best of our knowledge, almost all the fluoropolymer nanocomposites in the literature are based on the use of nanoclay. Nanoclay was found to affect vulcanization kinetics of a fluoroelastomer. It could effectively reduce the energy requirement for the curing process of the fluoroelastomer (Kader and Nah 2004) and increase the thermal degradation temperature of the fluoroelastomer in both nitrogen and oxygen atmospheres (Kader, et al. 2006). Likozar et al. (2007) simulated dynamic mechanical properties of a vulcanized fluoroelastomer and showed the viscoelastic behaviors of the fluoroelastomer at different temperatures.

Compared to other polymer nanocomposites, fluoropolymer nanocomposites have received significantly less investigations. The influences of the nanofillers and their surface treatments on the vulcanization of fluoroelastomers and the mechanical, electrical, and thermal properties of the vulcanized nanocomposites are still not clear. Fluoropolymer-graphene nanocomposites have not been reported elsewhere in the

literature. Considering the unique properties of fluoropolymers and their important roles in many demanding applications, detailed investigation of fluoropolymer nanocomposites is needed to optimize their processing methods and understand their vulcanization mechanisms and morphology-property relationships.

The fluoroelastomer used in this study was a dipolymer of vinylidene fluoride and hexafluoropropylene (VDF-HFP) which was vulcanizable with peroxide. Fluoroelastomer vulcanization in the presence of different nanofillers was performed and different formulations of FKM nanocomposites were obtained through intensive mixing in a torque rheometer. The object of this work is to study:

- (1) Factors influencing the curing and vulcanization kinetics of FKM nanocomposites,
- (2) Morphology of the FKM nanocomposites
- (3) Effects of different nanofillers on thermal, mechanical and dynamic mechanical properties of the FKM nanocomposites,

2.3 Experimental

2.3.1 Materials

The fluoroelastomer (FC-2260, Dyneon LLC) was a copolymer of vinylidene fluoride and hexafluoropropylene (VDF-HFP). An organic peroxide, 2, 5-dimethyl-2, 5-di (t-butylperoxy)-hexane (DBPH-50), was used as the crosslinking agent for the fluoroelastomer and was obtained from R.T. Vanderbilt Company, Inc. Commercial organically modified nanoclay I.34TCN (hereafter “S-clay”) was purchased from Nanocor Inc. According to literature, this organo-nanoclay is prepared by treating original Montmorillonite clay with a quaternary ammonium salt type cationic surfactant.

The ammonium salt has two alkyl (tallow) tails and hydroxyl group attached to either the tallow tail or the ammonium head (Yang and Tsai 2007). Silicon dioxide nanoparticle (~10 nm) was purchased from Sigma-Aldrich, and graphite from Fisher Scientific. In addition, we also prepared the fluoroaliphatic quaternary ammonium fluorosurfactant (FS-1620, DuPont) treated nanoclay (designated as “FS-clay”) following the method in the literature (Thomassin et al. 2006). 3-aminopropyltriethoxysilane, a silane coupling agent used to treat silica was purchase from Acros Organics.

2.3.2 Silica and Graphite Treatments

Silica is usually treated with silane coupling agents to increase its interfacial bonding with polymer matrix and improve its dispersion in the matrix (Iijima, et al. 2007). Many factors affect the effects of silane treatment. Chaimberg and Cohen (1990) found that a two-step treatment method improved the amount of chemisorbed coupling agents, with the degree of improvement depending on the pH value of the treatment environment. Kamiya et al. (2004) reported that the diameter of silica particles significantly affected their surface properties. In this thesis study, a silane application guide from the producer of the agent was followed (Advanced Polymer, INC., 2009). The treatment environment was kept pH neutral. The concentration of the aqueous silane solution was 3.5%. The amount of required silane was calculated based on the following equation:

$$M=m * A / A_c$$

where M is the amount of silane, m is amount of silica, A is the surface area of silica and A_c is the minimum coating area of silane coupling agent. In our study, the surface area of

silica equals to $7\text{m}^2/\text{g}$ and minimum coating area of the used amino-silane is $353\text{ m}^2/\text{g}$ (Advanced Polymer, INC., 2009).

Silica was first dispersed in distilled water and then silane was slowly added to the suspension until the required silane concentration and amount were reached. The suspension was stirred for 24 h at room temperature and the treated silica was separated by centrifuge and dried at $100\text{ }^\circ\text{C}$ for 3 h. This treated silica (T-SiO₂) was used as one of the nanofillers for the preparation of fluoroelastomer nanocomposites.

Natural graphite flake can be turned into functionalized graphene single sheets through oxidation in a mixture of concentrated sulfuric acid and concentrated nitric acid and then followed by rapid thermal exfoliation (Schniepp, et al. 2006). McAllister et al. (2007) reported similar method to produce single sheet functionalized graphene by oxidation and thermal expansion of graphite. We followed this oxidation and expansion method and the following steps were used to process graphite flake to produce treated graphite (T-G) (McAllister, et al. 2007)

1. prepare sulfuric acid (98.0%) and nitric acid (63.0%) mixture (4:1 v/v),
2. add graphite flake into the mixture and stirred the suspension continuously for 16 hours at room temperature,
4. wash the sample with distilled water until neutralization was reached,
5. dry the sample at $100\text{ }^\circ\text{C}$ in a convection oven,
6. heat the dried sample at $1050\text{ }^\circ\text{C}$ for 45s for fast expansion.

The obtained TG was used to prepare fluoroelastomer nanocomposites.

2.3.3 Study of Vulcanization by Torque Rheometry and DSC

Torque rheometry and DSC are the two most commonly used methods to determine the curing reaction and cure kinetics for a thermosetting system (Kader and Nah 2004). The fluoroelastomer FC2260 used in this study requires two curing stages: initial low temperature curing during mixing and post curing at a higher temperature. The initial curing of the FC2260 nanocomposites was studied by a torque rheometer (Haake Rheomix 600 with a mixing head of 69-mL net chamber capacity). The optimal sample weight for the highest mixing efficacy can be determined by the following equation (Rozman, et al. 2001):

$$M = \rho * V_n * 0.7$$

where M is sample weight, ρ is melt density, and V_n is net chamber volume.

60 grams of the FC2260 and the nanofiller was first added into the mixing head of the Haake rheometer equipped with a pair of mixing rotors. The elastomer and nanofiller were mixed at 80 rpm and 177 °C for 3min, followed by the addition of the curing agent, DBPH-50, and the mixing was then continued for another 12 minutes. The change of mixing torque with time was recorded and used to assess the vulcanization behaviors of the FC2260 nanocomposites.

The post curing of the nanofiller filled FC2260 was studied using DSC. A typical rubber vulcanization process involves multiple and complex reactions. Models have been developed to depict the reaction process and give insight to the vulcanization mechanisms. Two types of kinetic models based on DSC measurement, applicable to isothermal and

non-isothermal vulcanization, respectively, have been developed. For isothermal vulcanization, the model developed by (Lopez-Manchado, et al. 2003) can be used:

$$d\alpha / dt = K(T)\alpha^m(1-\alpha)^n$$

where $d\alpha / dt$ is the vulcanization rate, with α , degree of curing, and t , the time. K is the specific rate constant at temperature T and m and n are both the order of reaction.

For non-isothermal vulcanization, the reaction can be quantified by Kissinger's theory (Kissinger 1957):

$$-\ln(q/T_p^2) = E_a/RT_p - \ln(AR/E_a)$$

where q is the heating rate, T_p is the exothermic peak temperature, E_a is the activation energy, R is the gas constant, and A is a pre-exponential factor. A plot of $-\ln(q/T_p^2)$ versus $1/T_p$ should be linear and the apparent activation energy can be obtained from the slope of the straight line.

In this study, non-isothermal kinetic model was used to study the vulcanization kinetics of the FC2260 nanocomposites. DSC analysis of those materials mixed by the Haake mixing head (i.e. after initial vulcanization) was performed using a Mettler-Toledo 822e DSC. Each sample was tested using four different heating rates, i.e. 8, 10, 15, and 20 °C/ min. The collected data was used to analyze vulcanization kinetics of FC2260 in the nanocomposites.

2.3.4 Other Characterizations

Post curing of the FC2260 and its nanocomposites was performed by pressing mixed material into sheet (1.5 mm × 40mm × 40mm) at 242 °C using a compression mold and a hot press machine (Model 3851-0, Carver Inc.). The temperature and press pressure (2×10^3 psi) were maintained for 24 h to make sure the fluoroelastomer was fully cured (Dyneon technical information). The obtained sheets were used for further characterizations. The formulations of all the prepared FC2260 nanocomposites are listed in Table 2.1.

Dynamic mechanical analysis (DMA) was carried out on a DMA Q800 dynamic mechanical analyzer (TA instruments) using a single cantilever configuration. Samples for DMA measuring were cut from above prepared sheets of fully cured FC2260 nanocomposites. All samples were tested from -60 to 120 °C at a ramp rate of 3 °C/min and a frequency of 1 Hz. Oscillating strain was set at 0.02% for all tests.

Table 2.1 Formulations of fluoroelastomer nanocomposites

Samples	Compositions
Neat FC2660	FC 2260 + 2.5% Curing Agent ^a
FC 2260/S-clay	FC 2260 + 2.5% Curing Agent + 2% S-clay ^b (FC 2260/ 2%S-clay)
	FC 2260 + 2.5% Curing Agent + 4% S-clay (FC 2260/ 4%S-clay)
FC 2260/FS-clay	FC 2260 + 2.5% Curing Agent + 2% FS-clay (FC 2260/ 2% FS-clay)
	FC 2260 + 2.5% Curing Agent + 4% FS-clay (FC 2260/ 4% FS-clay)
FC 2260/UT-SiO ₂	FC 2260 + 2.5% Curing Agent + 2% untreated silica (FC 2260/ 2% UT-SiO ₂)
	FC 2260 + 2.5% Curing Agent + 4% untreated silica (FC 2260/ 4% UT-SiO ₂)
FC 2260/ T-SiO ₂	FC 2260 + 2.5% Curing Agent + 2% treated silica (FC 2260/ 2% T-SiO ₂)
	FC 2260 + 2.5% Curing Agent + 4% treated silica (FC 2260/ 4% T-SiO ₂)
FC 2260/T-G	FC 2260 + 2.5% Curing Agent + 2% treated graphite (FC 2260/ 2% T-G)
	FC 2260 + 2.5% Curing Agent + 4% treated graphite (FC 2260/ 4% T-G)

a. Curing agent content was based on the weight of fluoroelastomer.

b. Nanofiller content was based on the weight of fluoroelastomer.



Figure 2.1 Tensile testing set-up with the tensile strain measured by a laser extensometer

Thermogravimetric analysis (TGA) was performed on a SDT Q600 thermogravimetric analyzer (TA instruments). The test samples were scanned from 30 to 800 °C at a heating rate of 20 °C/min under continuous nitrogen flow. The temperature corresponding to a 5% weight loss was taken as the degradation onset temperature (T_{onset}).

For tensile test, dumbbell-shaped specimens were prepared with a Type IV (ASTM D638) sample cutter and tested according to ASTM D 638–91. Five replicates for each formulation were tested using an Instron 4466 (capacity 500 N) at a crosshead speed of 10 mm/min. Tensile strain were monitored by an EIR laser extensometer (model LE-05). The setup for the tensile testing is shown in Figure 2.1.

The dispersion of the nanofillers and the morphology of the fluoroelastomer nanocomposites were studied by a transmission electron microscope (TEM) (JEOL 1200EX) operating at 100 kV. Thin slices (80-100 nm) of the samples were cut using an ultramicrotome (Powertome X, Boeckeler Instrument) at -50 °C. The thin slices floated in alcohol after cutting and were collected using TEM copper grids. The cryo-sliced surface was also examined by Field Emission Scanning Electron Microscopy (FE SEM, Quanta 200F) to investigate the morphology of fluoroelastomer nanocomposites. In order to better understand the phase structures of the composites, samples were also cryo-fractured in liquid nitrogen and the fracture surfaces were examined by FE SEM.

2.4 Results and Discussion

2.4.1 Factors Influencing Curing Behaviors of Fluoroelastomer Nanocomposites

The fluoroelastomer FC2260 used in this study has a two-stage curing process including a initial curing stage for 7-20 minutes at 177 °C and a post curing stage for 20-24 h at 242 °C. Figure 2.2 compares the Haake mixing torque of the different FC2260 nanocomposites during the initial curing stage. The mixing torque decreased rapidly and gradually leveled off as the elastomer was melted and mixed with the nanofillers toward higher homogeneity. The crosslinking agent was added after three minutes of mixing, and the mixing torque increased significantly, indicating the occurrence of the elastomer crosslinking. Figure 2.2 (a) shows that, before adding the crosslinking agent, the higher the treated silica (T-SiO₂) content, the larger the mixing torque. This was due to the viscosity increase of the elastomer caused by the added nanofiller. Before the curing agent was added, the difference in mixing torque between samples containing 0, 2, and

4% T-SiO₂ was relatively small. After adding the crosslinking agent, the difference was remarkably increased, implying that there existed another factor causing the torque difference on the initial curing stage. This factor was believed to be the amino-silane coupling agent used to treat silica. Besides peroxide curing agent, diamines can also cure fluoroelastomers (Beck, et al. 2009). The amino groups on the surface of T-SiO₂ took part in the curing reaction, therefore, T-SiO₂ actually acted as a secondary crosslinking agent for the elastomer during the mixing. This additional crosslinking effect of T-SiO₂ led to the enlarged difference of the mixing torque.

Figure 2.2 (b) shows that the nanofiller type also played an important role in determining the mixing torque. Before adding the crosslinking agent, the neat fluoroelastomer (neat-FC2260) exhibited the lowest mixing torque. The modified clay (FS-clay) filled FC2260 showed the highest mixing torque before crosslinking. After adding the crosslinking agent, the order of the mixing torque was completely different. The treated graphite (T-G) filled FC2260 showed the lowest mixing torque, implying T-G hindered crosslinking reaction of the FC2260. In contrast, the T-SiO₂ filled FC2260 exhibited the highest mixing torque due to the role of T-SiO₂ as a secondary crosslinking agent for the elastomer. Following T-SiO₂, untreated silica (UT-SiO₂) and FS-clay led to the second and third highest mixing torque.

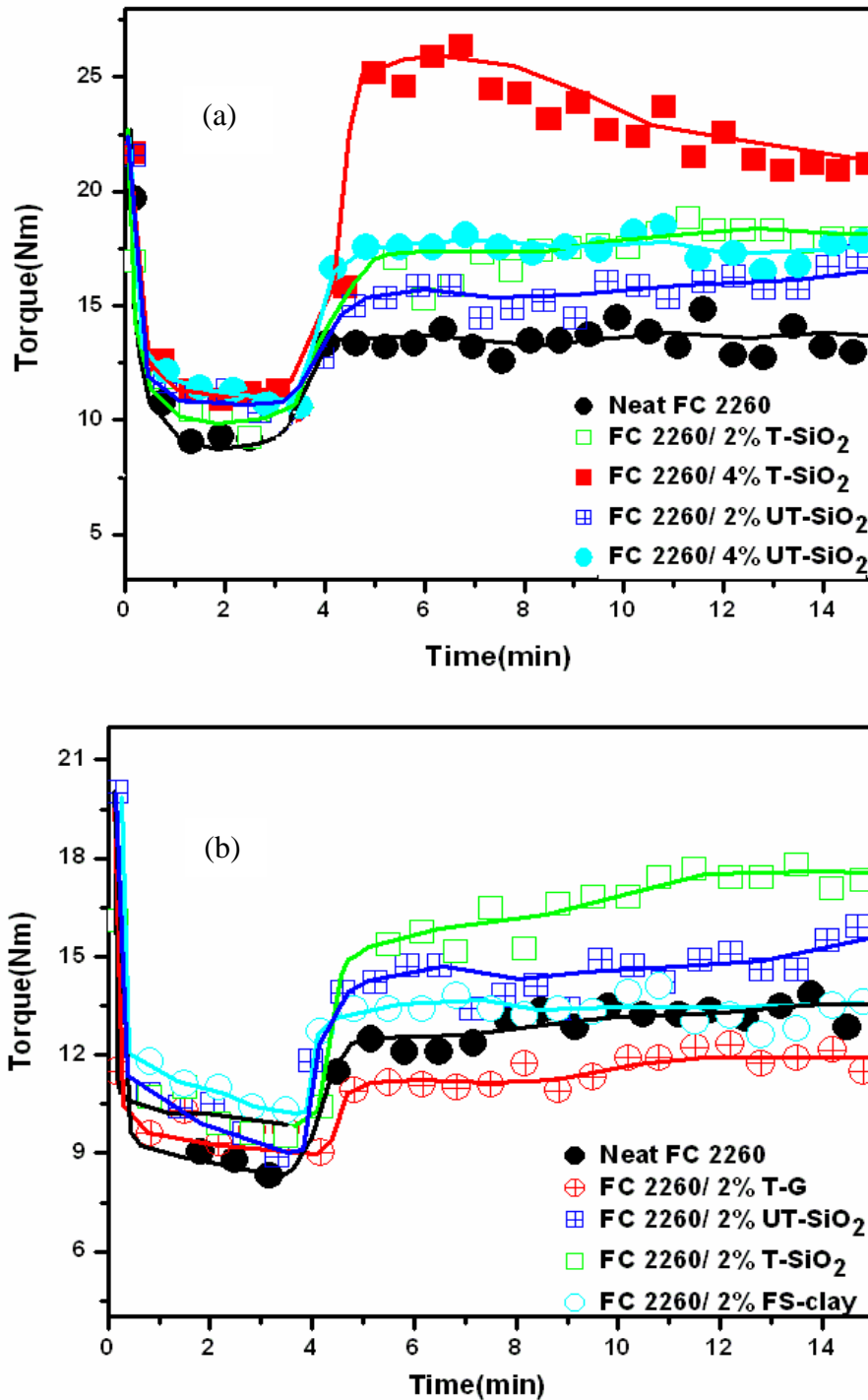


Figure 2.2 Mixing torque-time curves of FKM formulations: (a) different loading of treated silica and untreated silica in FKM at 177 °C, (b) effect of different nanofillers on the torque increase of the FKM nanocomposites

2.4.2 Vulcanization Kinetics during Post Cure

Study of vulcanization kinetics of FC 2260 and its nanocomposites was performed on the Haake rheometer premixed materials using DSC. Non-isothermal curing in DSC was carried out from 30 to 350 °C at the heating rates of 8, 10, 15, and 20 °C/min, respectively. Activation energy of the vulcanization was calculated using the Kissinger's equation. Figure 2.3 shows $-\ln(q/T_p^2)$ versus $1/T_p$ for the samples comprising treated silica and graphite. According to the equation, $-\ln(q/T_p^2)$ versus $1/T_p$ yields a linear relationship and the activation energy E_a , which is related to the mechanism of the curing process, is obtained from the slope of the $-\ln(q/T_p^2)$ versus $1/T_p$ line. Large slope means high activation energy and high resistance to the cultivation process. The values of E_a for all the samples are given in Table 2. As shown in Figure 2.3a, the addition of treated silica (T-SiO₂) reduced E_a of the neat FC 2260. E_a continuously decreased with increasing T-SiO₂ content, indicating that the treated silica facilitated the vulcanization of the fluoroelastomer. FC 2660 comprising 4% T-SiO₂ displayed the lowest activation energy (32.6 kJ/mol) among all the samples, which is in agreement with the results obtained from Haake mixing where FC 2660/ 4% T-SiO₂ exhibited the highest mixing torque. The promotion of the fluoroelastomer vulcanization by the T-SiO₂ is explained by its function as a secondary crosslinking agent. T-SiO₂ reduces the activation energy of neat FC 2660 from 81.0 kJ/mol to 65.1 and 32.6 kJ/mol for 2 and 4% T-SiO₂, respectively (Table 2). In comparison, 2 and 4% untreated silica reduced the activation energy to 72.3 and 67.8 kJ/mol, respectively. The higher activation energy of the T-SiO₂ composites (especially at 4% nanofiller content) again proved the crosslinking effect of the silane coupling agent.

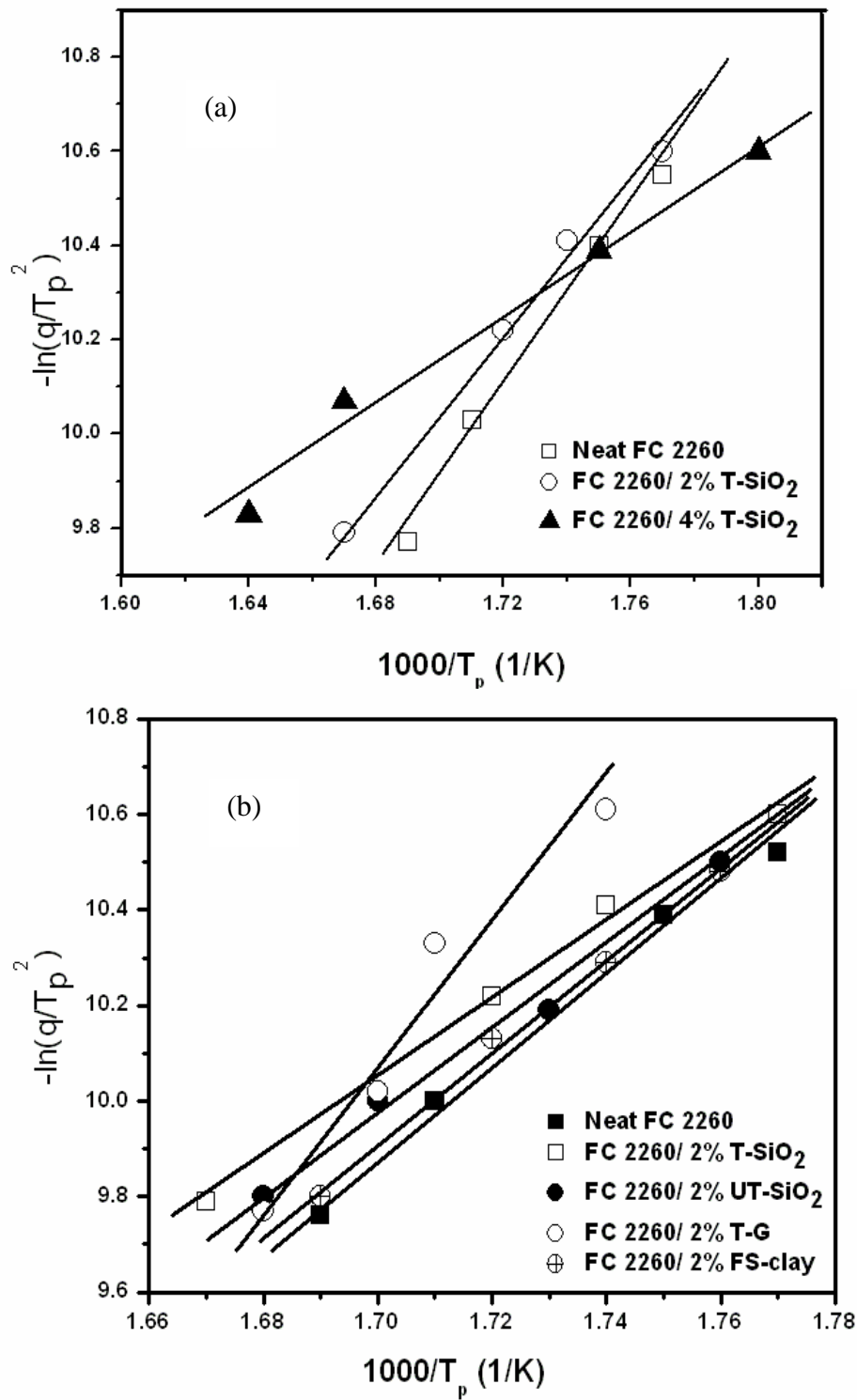


Figure 2.3 Calculation of activation energy from non-isothermal DSC data based on Kissinger equation.

Table 2.2 Thermal characteristics of fluoroelastomer nanocomposites

Samples	E_a^a (kJ/mol)	T_g^b (°C)	$T_{5\%}^c$ (°C)	T_{max}^d (°C)
Neat FC 2660	81.0	-10.0	452.3	492.4
FC 2660/ 2% S-clay	75.3	-8.5	425.7	475.0
FC 2660/ 4% S-clay	64.5	-8.2	410.0	469.5
FC 2660/ 2% FS-clay	71.1	-6.9	440.7	489.2
FC 2660/ 4% FS-clay	69.2	-3.2	434.9	470.6
FC 2660/ 2% T-G	127.0	-8.0	458.6	494.6
FC 2660/ 4% T-G	124.8	-7.4	454.8	495.1
FC 2660/ 2% UT-SiO ₂	72.3	-5.5	458.6	496.3
FC 2660/ 4% UT-SiO ₂	67.8	-5.0	466.3	496.5
FC 2660/ 2% T-SiO ₂	65.2	-3.9	460.8	498.7
FC 2660/ 4% T-SiO ₂	32.6	-3.0	471.1	500.8

a. E_a is activation energy; b. T_g is glass transition temperature; c. $T_{5\%}$ is onset degradation temperature; d. T_{max} is temperature of maximum degradation rate.

Nanoclay moderately reduced the activation energy of the fluoroelastomer in all four formulations (Table 2). Higher clay content led to slightly lower energy for both FS-clay and S-clay, while FS-clay showed a larger effect on reducing E_a than S-clay. Quaternary ammonium salt treated organoclay has been shown to decrease the activation energy of vulcanization and the reason has been ascribed to the accelerating effect of the quaternary ammonium salt (Paciorek, et al. 2003). FS-clay is also an organoclay prepared by treating original clay with a fluoroaliphatic quaternary ammonium, therefore, it is also able to accelerate the process. Moreover, the fluoroaliphatic tail of the ammonium on the surface of FS-clay increased its compatibility with the fluoroelastomer matrix, which improved the dispersion of FS-clay and therefore further promoted the vulcanization of the elastomer.

In contrast, T-G displayed the opposite effect on the vulcanization of the elastomer. The addition of T-G increased E_a from 81.0 kJ/mol to 127.0 (2% T-G) and 124.8 kJ/mol (4% T-G), indicating that T-G hindered elastomer vulcanization. This result was consistent with the mixing torque results which showed that the FC 2660/T-G blend has the lowest mixing torque among all the samples (Figure 2.2). The reason for T-G's hindrance to the elastomer vulcanization is not clear yet.

2.4.3 Dynamic Mechanical Properties

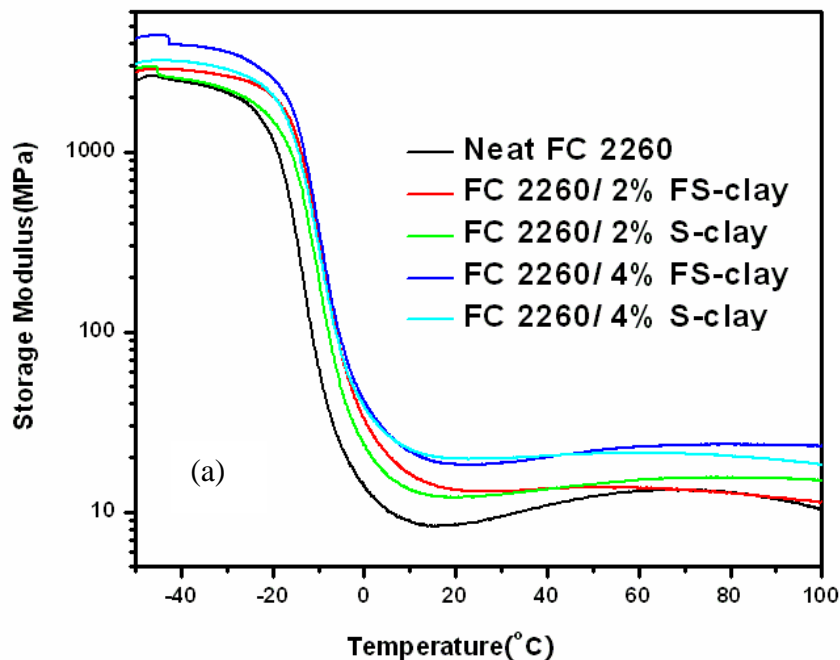
DMA measurements are often used to evaluate polymer stiffness under dynamic mode, molecular segment mobility, and maximum damping temperature (T_g) (Chartoff, et al. 2009). The glass transition temperature, T_g , represents a critical transition temperature for many polymers, as physical properties change drastically when the material transit from a hard glassy state to a rubbery state. Large segments of polymer chains start cooperative movement when the polymer reaches its glass transition temperature. In general, more heavily crosslinked rubber leads to higher T_g because the structure of three dimensional network hinders large scale chain movement. The T_g of highly crosslinked materials can not be easily detected by DSC since the amount of heat exchange is small during the transition, but can be easily measured by DMA because DMA is 10 to 100 times more sensitive than DSC to the movement of polymer chains under dynamic bending mode (Menard 2008). Figure 2.4 shows the effects of various nanofillers on the storage modulus of FC2260 nanocomposites. Figure 2.4a compares the effects of the two types of clay on the modulus of the nanocomposites. The modulus plummeted at ca. -10°C due to glass transition of the fluoroelastomer. The modulus increased with the

content of the clay within the whole temperature range for both types of clay. However, at the same clay content FS-clay resulted in higher modulus of the composites than S-clay. This was attributed to FS-clay's higher compatibility with the fluoroelastomer matrix compared to S-clay, due to the former's treatment by a fluoroaliphatic quaternary ammonium fluorosurfactant. This increased compatibility led to better dispersion of the clay and stronger interfacial bonding between the clay and the matrix.

Figure 2.4b compares the modulus of neat FC 2260 and its nanocomposites containing 2% nanofillers. The neat FC 2260 displayed the lowest modulus among all the samples. In other words, all the tested nanofillers stiffened the elastomer. FC 2260/ 2% T-SiO₂ exhibited the highest modulus among the samples and FS-clay, T-G, and UT-SiO₂ filled FC 2260 nanocomposites had their modulus curves lying between those of the neat FC 2260 and FC 2260/2% T-SiO₂. The highest modulus for FC 2260/ 2% T-SiO₂ was the result of T-SiO₂'s crosslinking effect.

Figure 2.4c compares the modulus of the FC 2260 nanocomposites containing 4% nanofillers. The highest modulus for 2% nanofiller content, e.g. the modulus of FC 2260/ 2% T-SiO₂, was also drawn for comparison. This figure shows that higher nanofiller content led to higher composite modulus. The modulus of FC 2260/ 2% T-SiO₂ was almost the lowest one in Figure 2.4c. However, FC 2260/ 4% T-SiO₂ still exhibited the highest modulus, especially after the glass transition of the elastomer when the modulus of the samples is crucially determined by the crosslink density. For the same reason, T-G filled FC 2260 nanocomposites exhibited the lowest storage modulus (Figure 2.4b and c) above elastomer T_g , due to the hindrance of T-G to the elastomer vulcanization.

The glass transition temperature (T_g) of each sample is listed in Table 2.2. All the nanocomposites showed increased T_g due to the restricted mobility of the elastomer chain segments. There could be two reasons for the restricted chain segment movements. First, the elastomer chains physically attached to nanofiller surface led to reduced mobility. Second, the nanofillers which took part in the crosslinking reactions increased crosslink density of the elastomer and hence decreased the elastomer chain mobility. Among all the nanofillers, FS-clay and T-SiO₂ caused the most significant increase in the elastomer T_g (Table 2.2). For FS-clay, the fluorosurfactant on FS-clay surface increased the compatibility and interfacial bonding between clay and elastomer, which in turn increased the restriction to elastomer chain mobility. For T-SiO₂, the elastomer chains were chemically bonded to the nanofiller and the crosslink density of the elastomer was also increased. Therefore, T-SiO₂ showed even higher restriction to the chain mobility than FS-clay. As a result, T-SiO₂ led to a larger increase in elastomer T_g compared to FS-clay. The other nanofillers, i.e. S-clay, T-G, and UT-SiO₂, caused smaller increase in T_g due to their lack of strong interactions with the elastomer.



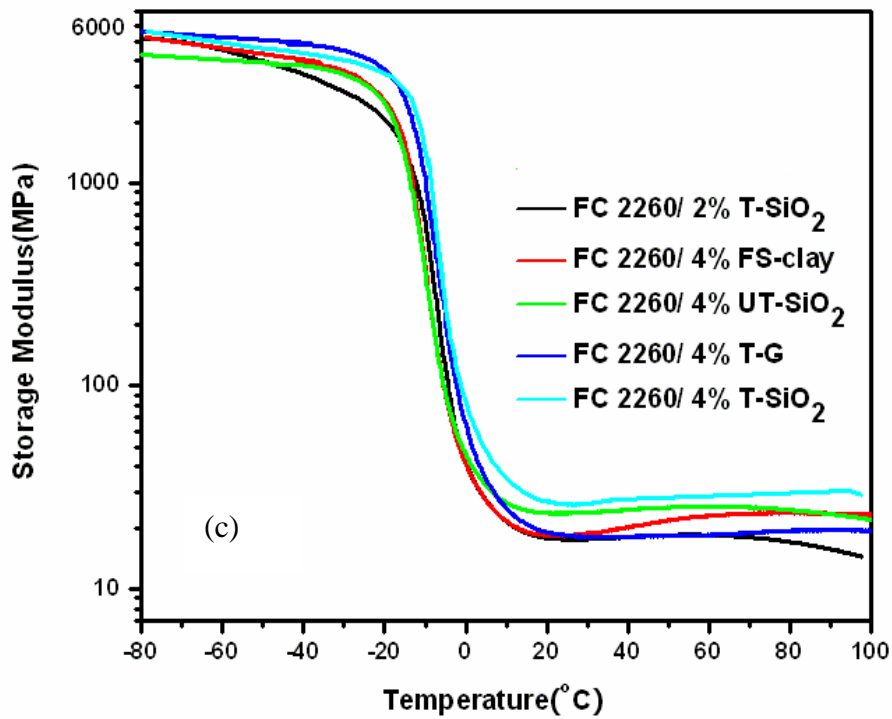
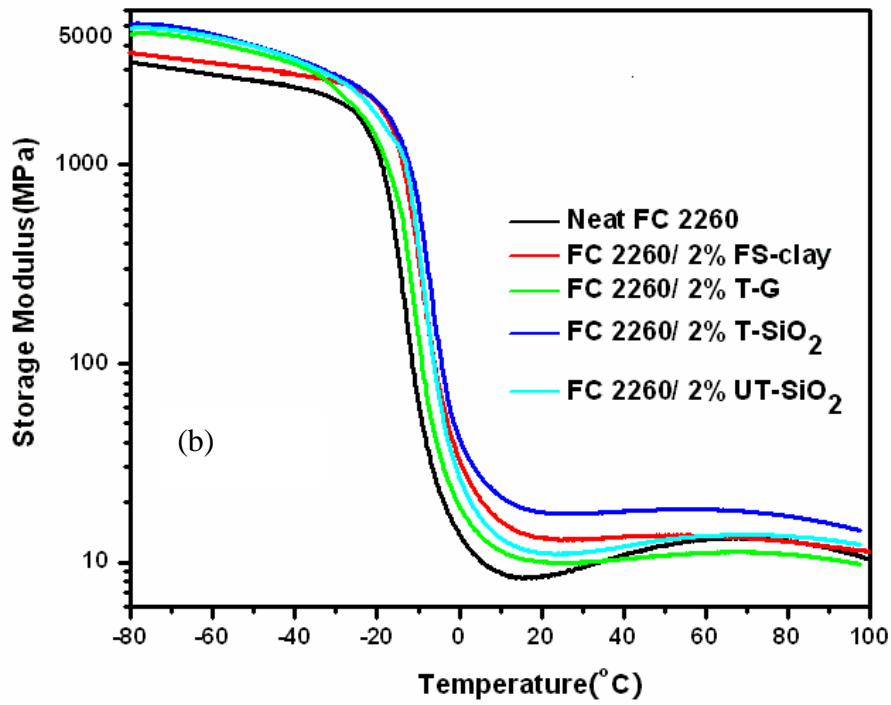


Figure 2.4 Storage modulus for different formulations of FKM nanocomposites.

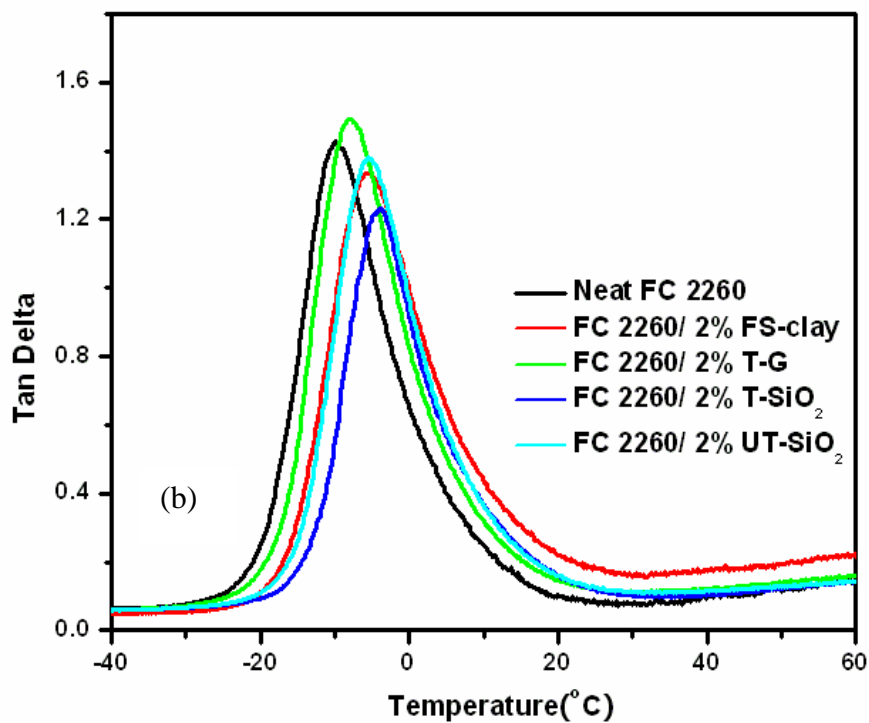
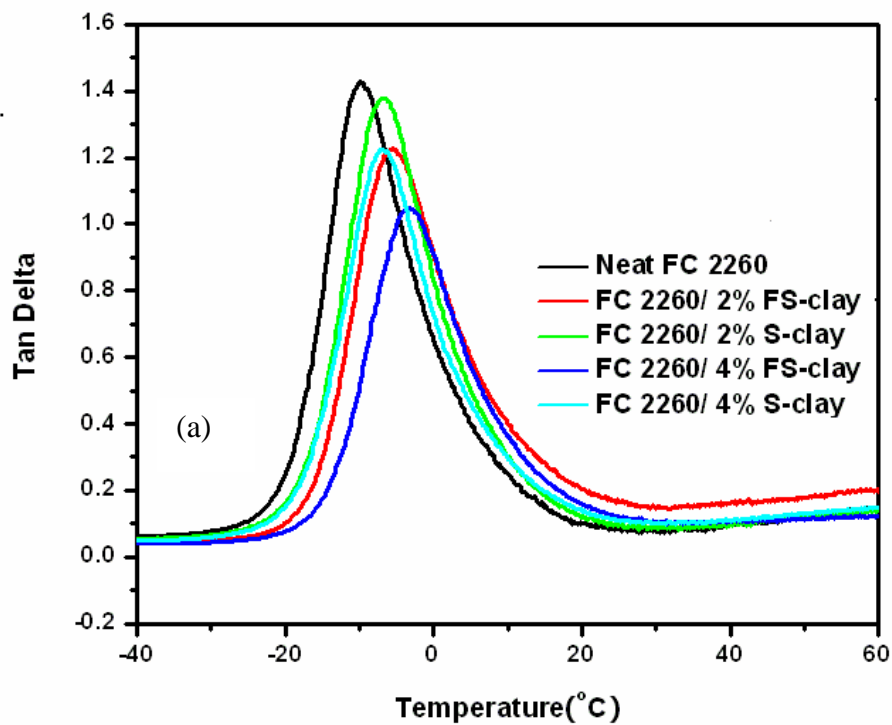


Figure 2.5 Damping peaks of different formulations of FKM nanocomposites.

2.4.4 Tensile Properties

Nanofillers have shown significant influences on the vulcanization of FC 2260 and the morphology of FC 2260 nanocomposites. Therefore, mechanical properties such as tensile strength and tensile modulus are expected to be significantly changed too. Figure 2.6 compares the tensile strength and tensile modulus of the FC 2260 nanocomposites. The addition of the nanofillers increased the tensile strength and modulus of FC 2260, regardless of the nanofiller type and content. For every type of the nanofillers, higher nanofiller content resulted in larger increase in the tensile properties.

FS-clay exhibited higher reinforcing effect on both strength and modulus than S-clay because of FS-clay's higher compatibility with the elastomer matrix and stronger promotion on the elastomer vulcanization. The same comparison is found between T-SiO₂ and UT-SiO₂. T-SiO₂ reinforced nanocomposites show significantly higher properties compared to UT-SiO₂ reinforced ones due to the former's higher compatibility and stronger promotion on the vulcanization. Indeed, T-SiO₂ reinforced nanocomposites displayed the highest strength and modulus among all the formulations. The chemical bonding between the T-SiO₂ and the fluoroelastomer facilitated T-SiO₂ dispersion and increased interfacial bonding between the two phases. Moreover, the addition of T-SiO₂ promoted elastomer vulcanization and increased crosslink density. These two factors contributed to the composite's exceptional mechanical properties.

T-G also markedly increased the tensile strength and modulus of the elastomer (Figure 2.6). Further increasing T-G content from 2 to 4% only slightly improved the properties, which may be due to particle aggregation at high T-G content. All the tensile properties of each formulation were listed in Table 3.

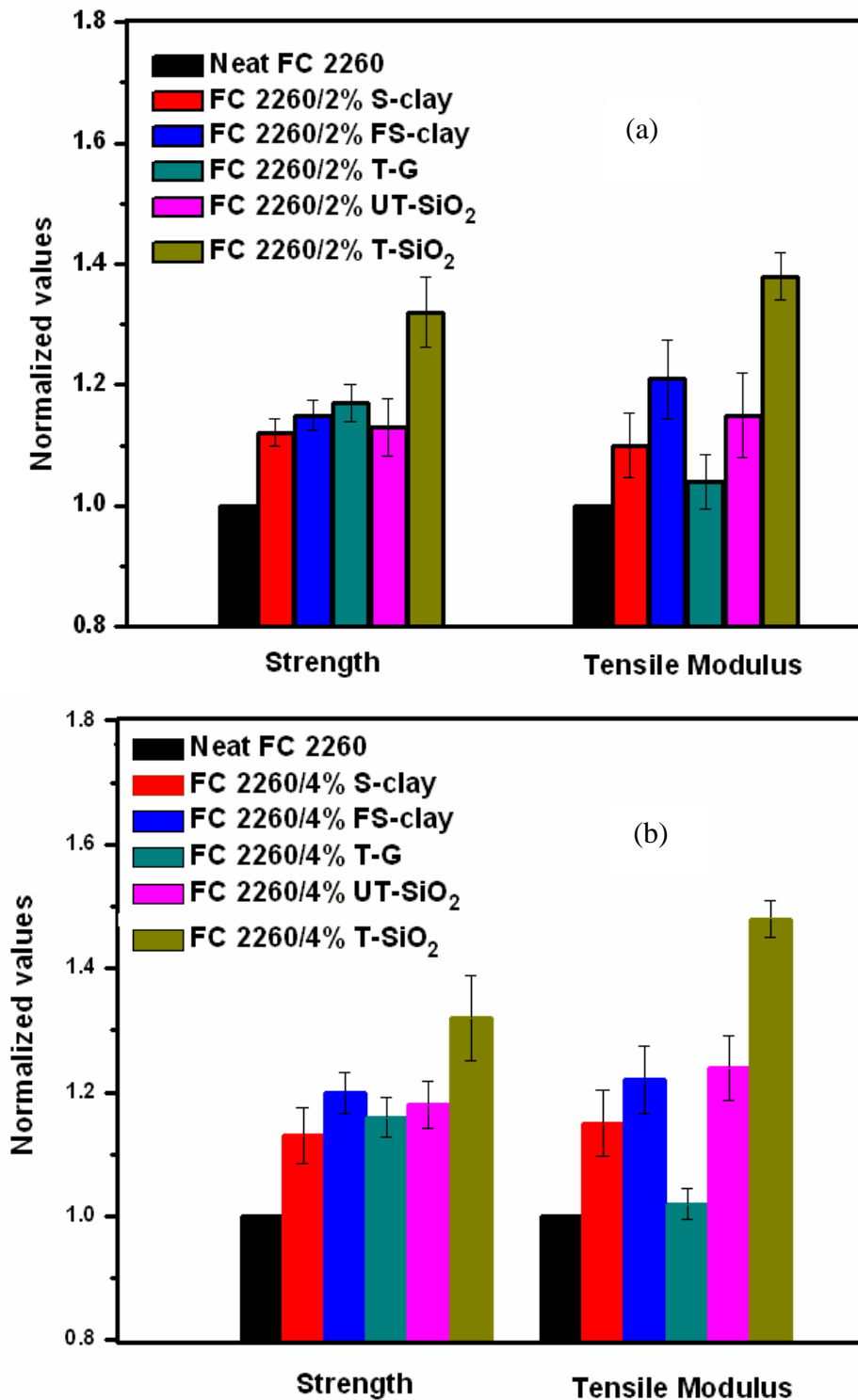


Figure 2.6 Tensile properties of the FKM nanocomposites comprising different types of nanofillers. (a) 2% nanofiller, (b) 4% nanofiller.

Table 2.3 Tensile properties of FC 2260 nanocomposites

Samples	tensile strength ^a (MPa)	modulus of elasticity (MPa)	elongation at break (%)
Neat FC 2660	4.6 ± 0.1	5.5 ± 0.1	1225 ± 85.0
FC 2660/ 2% S-clay	5.3 ± 0.1	6.0 ± 0.3	1136 ± 101.2
FC 2660/ 4% S-clay	5.5 ± 0.3	6.4 ± 0.3	1241 ± 179.1
FC 2660/ 2% FS-clay	5.4 ± 0.1	6.6 ± 0.3	1217 ± 115.6
FC 2660/ 4% FS-clay	5.6 ± 0.2	6.7 ± 0.2	1245 ± 110.2
FC 2660/ 2% T-G	5.5 ± 0.2	5.8 ± 0.1	1129 ± 98.5
FC 2660/ 4% T-G	5.4 ± 0.2	5.8 ± 0.1	1135 ± 55.8
FC 2660/ 2% UT-SiO ₂	5.3 ± 0.3	6.2 ± 0.3	1228 ± 72.6
FC 2660/ 4% UT-SiO ₂	5.5 ± 0.2	6.9 ± 0.2	1246 ± 88.4
FC 2660/ 2% T-SiO ₂	6.1 ± 0.3	7.6 ± 0.2	1271 ± 101.5
FC 2660/ 4% T-SiO ₂	6.3 ± 0.3	8.1 ± 0.1	1291 ± 64.5

a. Ultimate tensile strength of each formulation was used to characterize tensile strength

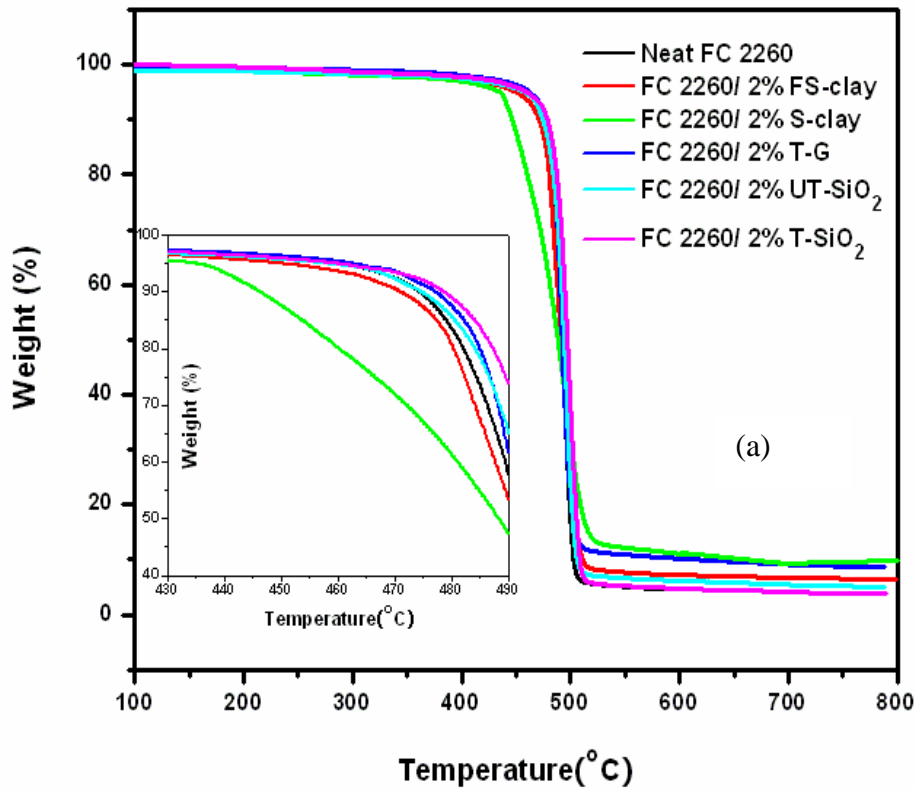
2.4.5 Thermal Stability

Fluoroelastomers in general show good thermal stability and their degradation temperatures are over 400 °C (Wang, et al. 2009; Maiti, et al. 2008). However, the applications in some special fields such as aerospace and energy related industries demand higher degradation temperatures. Effects of nanoclays on fluoroelastomer degradation temperature were investigated by M. Maiti et al. (2008). It was shown that the presence of unmodified nanoclays increased the degradation temperatures of FKM due to polymer-filler interaction, exfoliation, uniform dispersion and high thermal stability of nanoclays (Maiti, et al. 2008). The temperature at which 5% sample weight loss occurs ($T_{5\%}$) is considered as the degradation onset temperature. The temperature at which the highest weight loss rate occurs is set as the degradation temperature (T_{max}).

Both temperatures are used to compare the thermal stability of each formulation (Table 2). Figure 2.7a compares TGA weight loss curves of the neat FC 2260 and its nanocomposites comprising 2% nanofillers. It shows that the thermal stability of FC 2260 nanocomposites decreased with the addition of FS-clay and S-clay. This was especially true for S-clay, which lowered the $T_{5\%}$ from 452.3 °C for the neat FC 2260 to 425.7 °C for the nanocomposite containing 2% S-clay (Table 2). The addition of 4% of FS-clay or S-clay led to further decrease in the degradation temperature (Figure 2.7b and Table 2.2). Xie et al. (2001) indicated that the alkylammonium cations in the organoclay could decompose at elevated temperatures (150-300°C), and the decomposition products would catalyze the degradation of polymer matrixes, which led to earlier degradation of the materials. Moreover, the nanofillers of FS-clay and S-clay themselves were more prone to thermal degradation than the other three nanofillers. As shown in Figure 2.8, they exhibited a significantly larger weight loss than the other nanofillers at low temperatures (i.e. below the elastomer degradation temperature). These two factors together resulted in decreased $T_{5\%}$ for the nanocomposites comprising FS-clay and S-clay.

However, the influences of silica and graphite on the degradation temperature of the elastomer was opposite from that of the nanoclays. FC 2260/T-G, FC 2260/UT-SiO₂ and FC 2260/T-SiO₂ all exhibited different degrees of improvement in thermal stability compared with the neat FC 2260. The effect of treated graphite on improving thermal stability seemed very limited. The addition of 2% T-G only slightly increased $T_{5\%}$ of the elastomer (~ 2 °C increase), and 4% T-G only resulted an increase of ~ 6 °C in $T_{5\%}$. In contrast, silica nanoparticles, particularly the treated silica, greatly improved the thermal stability of the elastomer. While the addition of the untreated silica at 2 and 4 % loading

levels resulted in 6 and 14 °C increases in $T_{5\%}$, respectively, the addition of treated silica at 2 and 4% loading levels led to 18 and 29 °C, respectively. Again, the better interfacial adhesion and high degree of crosslinking were responsible for the high thermal stability in the latter case.



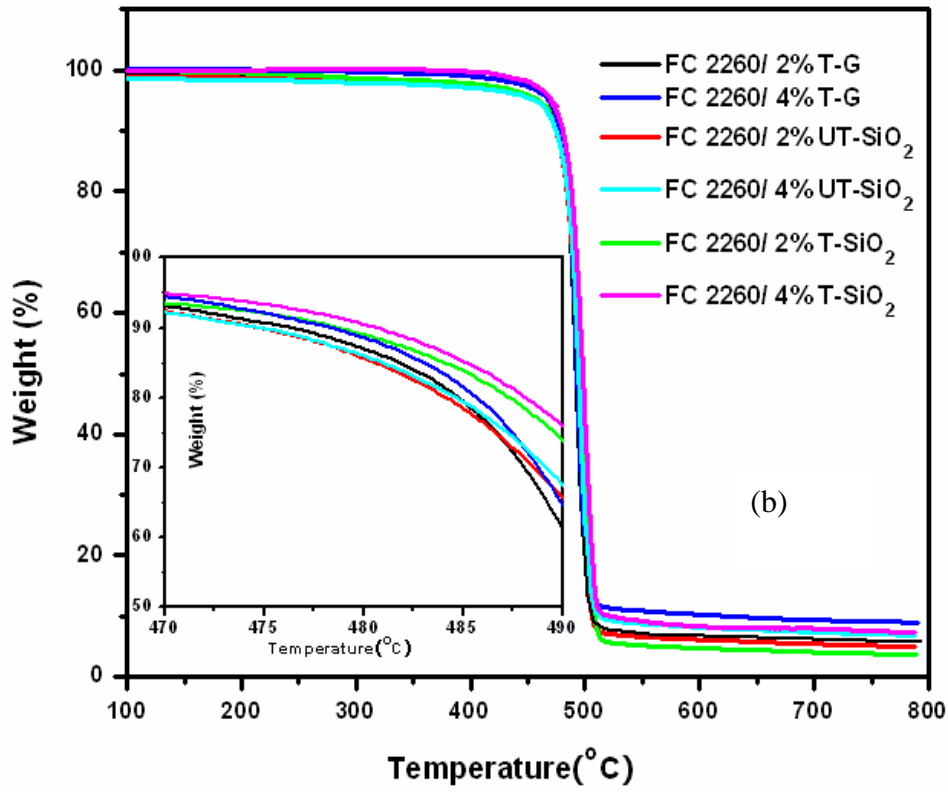


Figure 2.7 Representative TGA curves showing the effects of nanofillers on the thermal stability of FKM nanocomposites. (a) 2% different nanofillers, (b) comparison between 2 and 4% nanofiller contents.

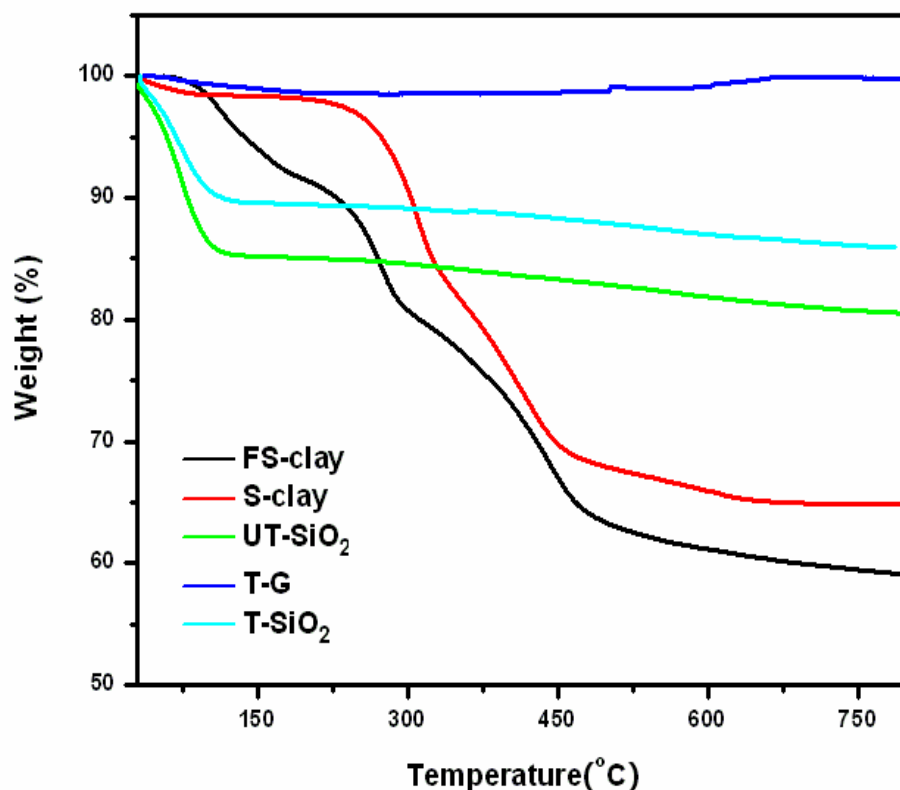
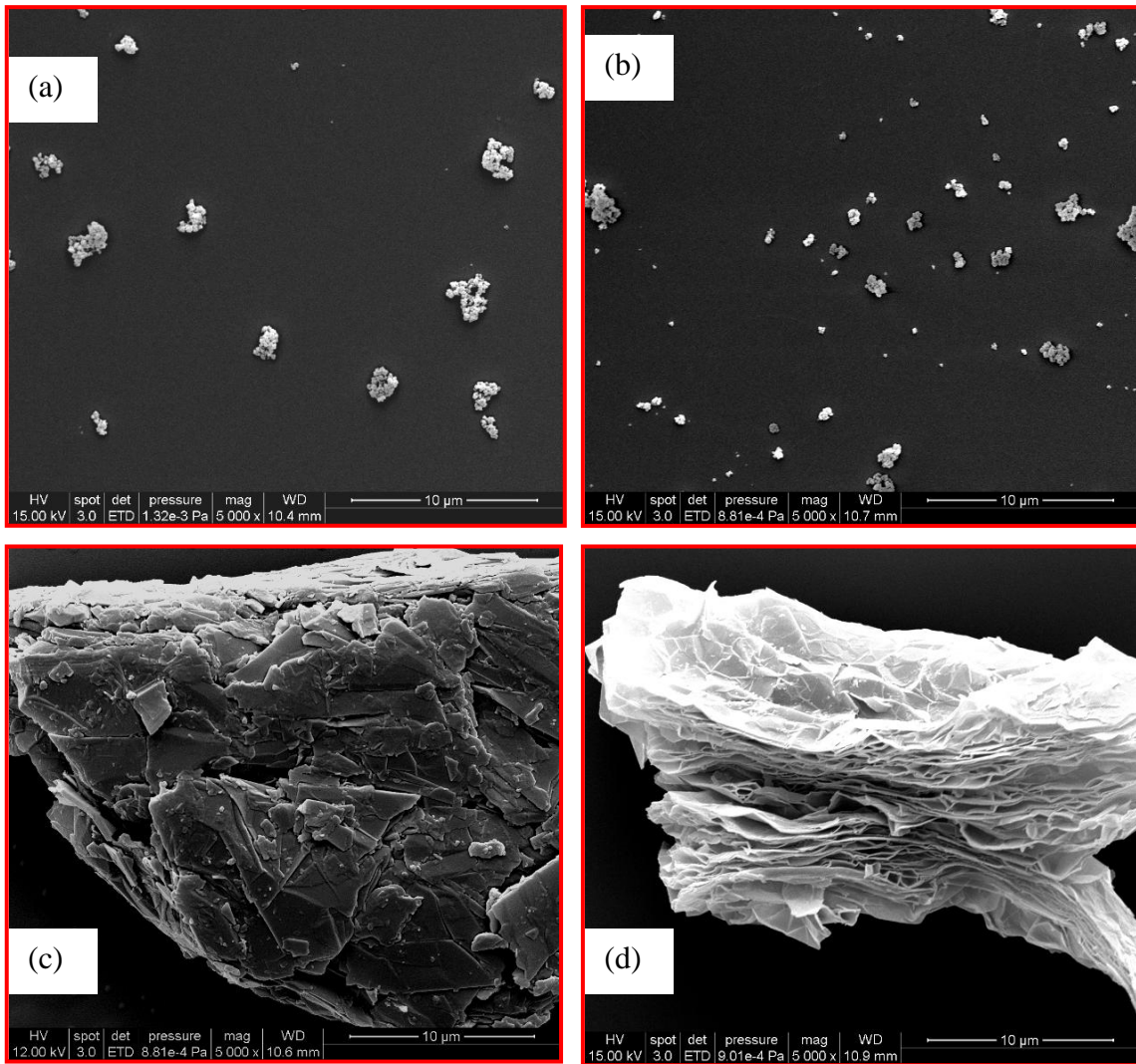


Figure 2.8 TGA curves showing weight loss of the different types of nanofillers.

2.4.6 Morphology of FC 2260 Nanocomposites

Figure 2.9 shows the SEM micrographs of silica and graphite before and after treatment. It is known that the received silica was nano-sized, the SEM images of T-SiO₂ and UT-SiO₂ suggest that both unmixed fillers existed as agglomerates. By comparing the micrographs of graphite before and after treatment (Figure 2.9c –e), it is clear that the graphite was effectively expanded as the layered structure revealed in the treated one. To examine the dispersion of the nanofillers in the elastomer and interaction between the nanofillers and the matrix, both cryo-fractured and cryo-sliced surfaces of the FC 2260/T-SiO₂, FC 2260/T-G and FC 2260-UT-SiO₂ composites were prepared for SEM

observations. Unfortunately, neither sample preparation methods offered the SEM observation with conclusive evidences on silica dispersion in the elastomer matrix, except the indications of more severe agglomeration of the nanofillers at 4% than at 2%. In contrast, the dispersion of the treated graphite in the matrix could be better noted. The stack of the wrinkled layers can still be recognized clearly in the micrographs, suggesting that the graphite was not delaminated or at least not fully delaminated.



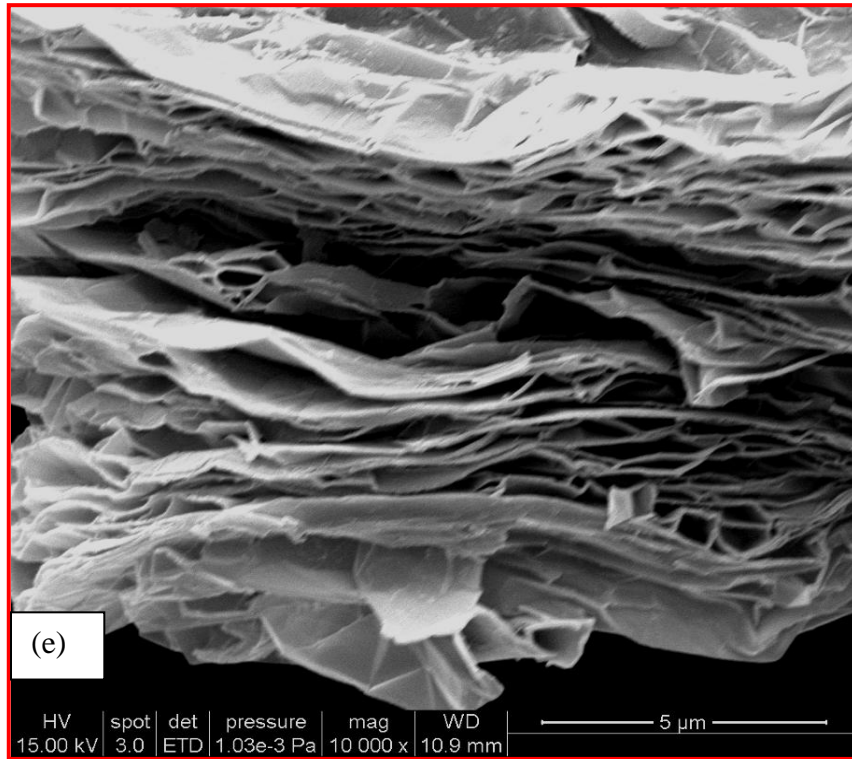
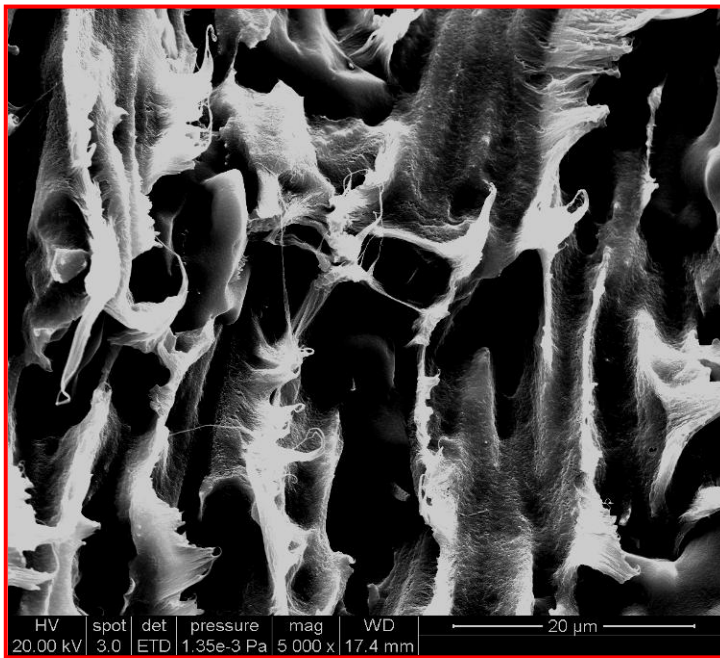
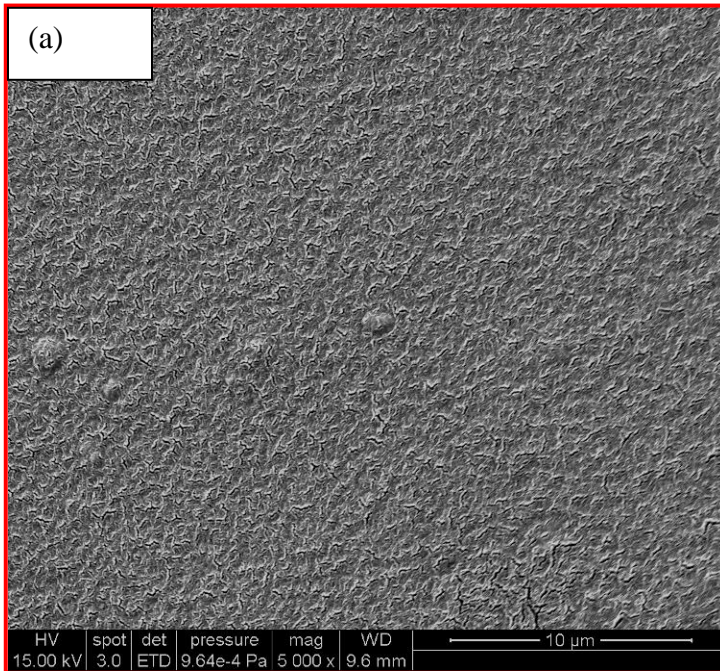
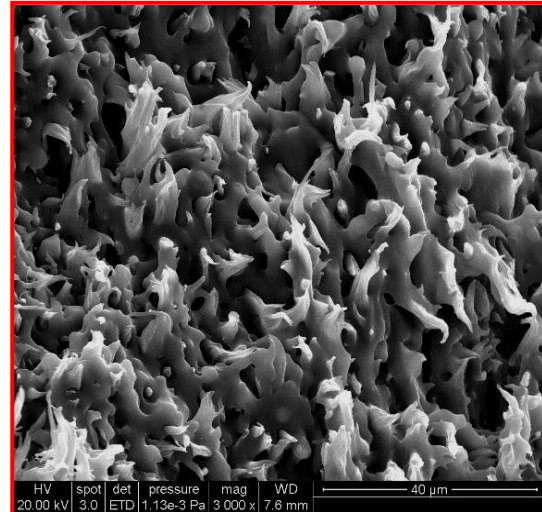
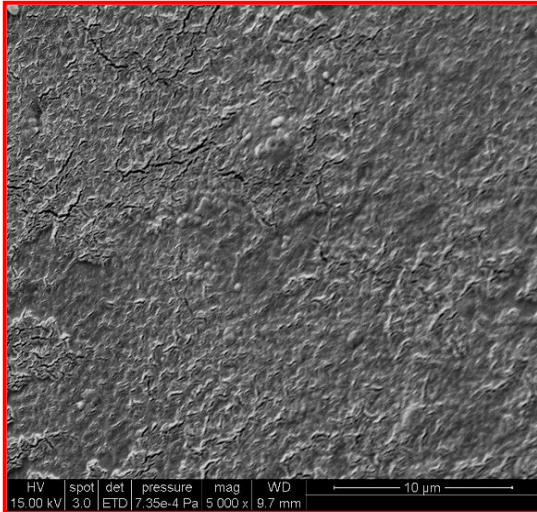
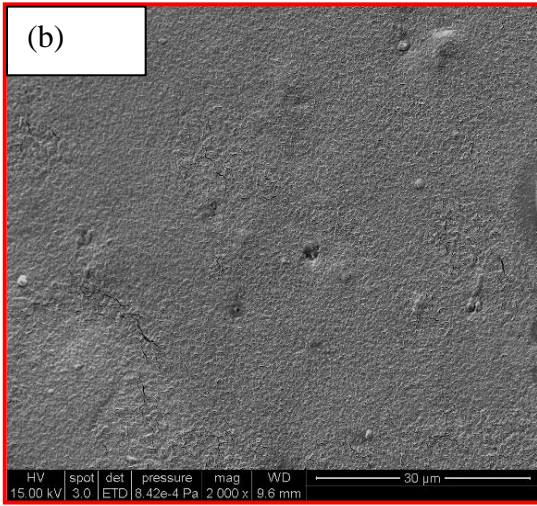
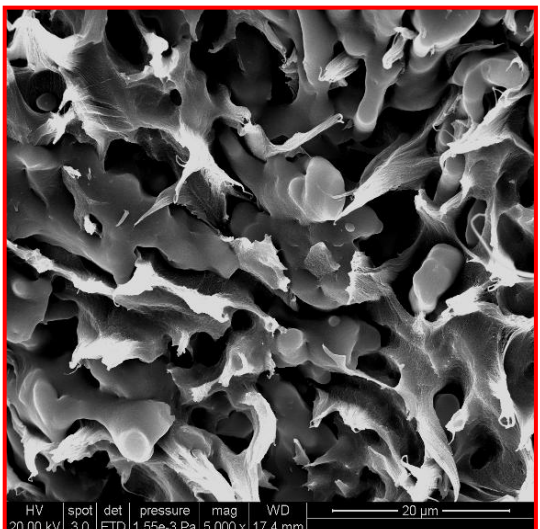
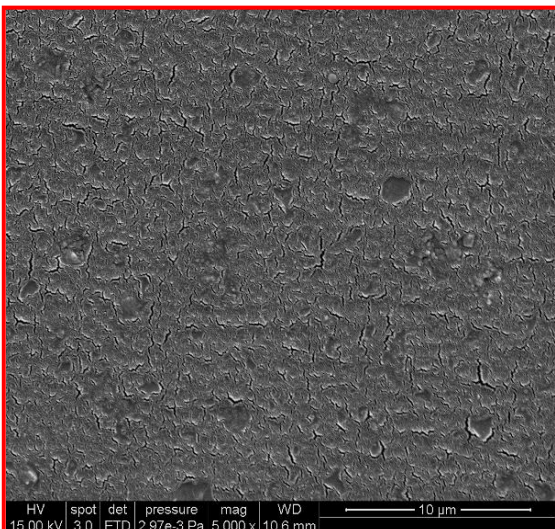
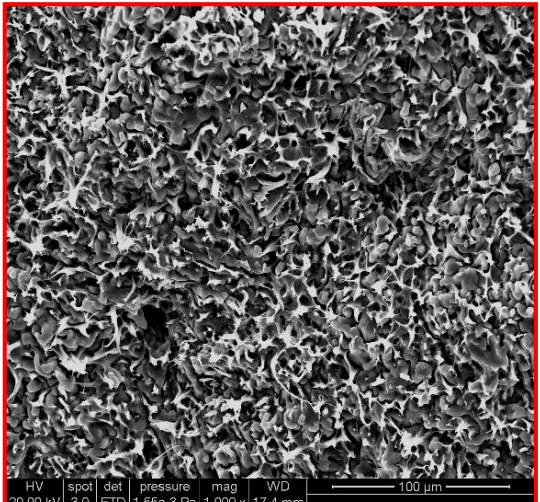
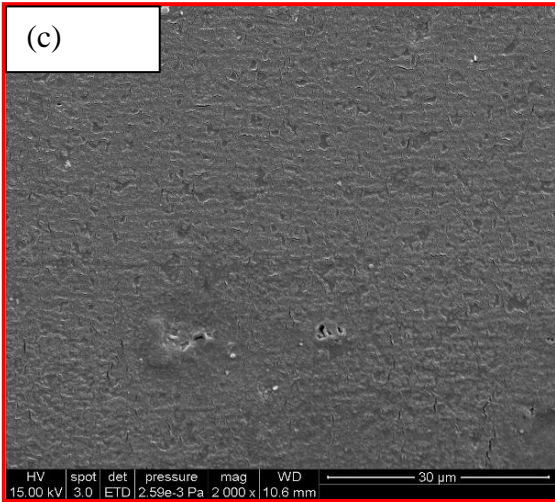


Figure 2.9 SEM images of treated silica (T-SiO₂) and treated graphite (T-G) compared to untreated silica (UT-SiO₂) and graphite flake. (a) UT-SiO₂, (b) T-SiO₂, (c) graphite, (d) and (e) T-G.







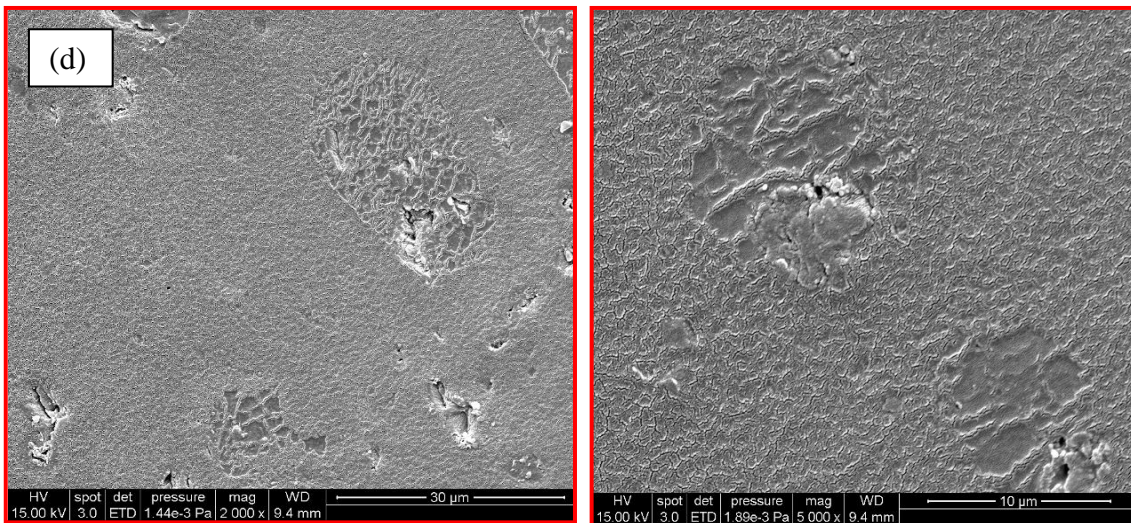


Figure 2.10 SEM images of FC 2260/UT-SiO₂, FC 2260/T-SiO₂ and FC 2260/T-G formulations.

- (a) cryo-sliced (top) and cryo-fractured (bottom) surfaces of neat FC 2260
- (b) cryo-sliced (left) and cryo-fractured (right) surfaces of FC 2260/2% UT-SiO₂
- (c) cryo-sliced (left) and cryo-fractured (right) surfaces of FC 2260/2% T-SiO₂
- (d) cryo-sliced surface of FC 2260/2% T-G.

2.5 Conclusions

In this chapter FKM nanocomposites comprising five types of nanofillers were successfully prepared. The effects of these nanofillers on the vulcanization behavior and curing kinetics of the elastomer were investigated. T-SiO₂, due to the amino groups on its surface, was able to take part in the crosslinking reaction of the elastomer and increase its crosslink density. As a result, it resulted in the highest mixing torque during the initial cure stage and the lowest activation energy during the post cure stage. T-SiO₂'s role as a secondary crosslinking agent offered its FKM nanocomposites the lowest damping and the highest mechanical properties, glass transition temperature, and thermal stability.

T-G was found to hinder elastomer curing because it led to the lowest mixing torque (even lower than that of the pure elastomer) and the highest activation energy (higher than that of the pure elastomer). Further investigation is required to find the reason.

FS-clay and S-clay caused remarkable decrease in the thermal stability of the elastomer. This was due to the ammonium salt surfactant attached to the clays, which decomposed at elevated temperature and the decomposition products catalyzed thermal decomposition of the elastomer.

All the tested nanofillers were found to increase the mechanical properties, glass transition temperature, and storage modulus of the elastomer. The degree of improvement depended on their interactions with the elastomer matrix and their effects on elastomer vulcanization.

2.6 Reference:

- Advanced Polymer, INC., 2005. “*Silane Coupling Agents*.”
- Balandin, A. A et al. 2008. “Superior thermal conductivity of single-layer graphene.” *Nano letters* 8:902–907.
- Beck, J. B et al. 2009. “Facile Preparation of Nanoparticles by Intramolecular Cross-Linking of Isocyanate Functionalized Copolymers.” *Macromolecules* 42:5629–5635.
- Chaimberg, M., and Y. Cohen. 1990. “Note on the silylation of inorganic oxide supports.” *Journal of colloid and interface science* 134:576–579.
- CHARTOFF, R. P, J. D MENCZEL, and S. H DILLMAN. 2009. “DYNAMIC MECHANICAL ANALYSIS (DMA).” *Thermal Analysis of Polymers, Fundamentals and Applications* 387.
- Chen, B. K, T. M Chiu, and S. Y Tsay. 2004. “Synthesis and characterization of polyimide/silica hybrid nanocomposites.” *Journal of Applied Polymer Science* 94:382–393.
- Das, B., K. E Prasad, U. Ramamurty, and C. N. R. Rao. 2009. “Nano-indentation studies on polymer matrix composites reinforced by few-layer graphene.” *Nanotechnology* 20:125705.
- Dikin, D. A et al. 2007. “Preparation and characterization of graphene oxide paper.” *Nature* 448:457–460.
- Geim, A. K., and K. S. Novoselov. 2007. “The rise of graphene.” *Nature materials* 6:183–191.
- Gianelli, W. et al. 2005. “Effect of matrix features on polypropylene layered silicate nanocomposites.” *Polymer* 46:7037–7046.
- Iijima, M., M. Tsukada, and H. Kamiya. 2007. “Effect of particle size on surface modification of silica nanoparticles by using silane coupling agents and their dispersion stability in methylethylketone.” *Journal of colloid and interface science* 307:418–424.
- Jiang, L., J. Zhang, and M. P Wolcott. 2007. “Comparison of polylactide/nano-sized calcium carbonate and polylactide/montmorillonite composites: Reinforcing effects and toughening mechanisms.” *Polymer* 48:7632–7644.
- Joly, S., G. Garnaud, R. Ollitrault, L. Bokobza, and J. E. Mark. 2002. “Organically

- modified layered silicates as reinforcing fillers for natural rubber.” *Chem. Mater* 14:4202–4208.
- Kader, M. A, M. Y Lyu, and C. Nah. 2006. “A study on melt processing and thermal properties of fluoroelastomer nanocomposites.” *Composites Science and Technology* 66:1431–1443.
- Kader, M. A, and C. Nah. 2004. “Influence of clay on the vulcanization kinetics of fluoroelastomer nanocomposites.” *Polymer* 45:2237–2247.
- Kamiya, H., M. Mitsui, H. Takano, and S. Miyazawa. 2004. “Influence of particle diameter on surface silanol structure, hydration forces, and aggregation behavior of alkoxide-derived silica particles.” *Journal of the American Ceramic Society* 83:287–293.
- Kim, G. M, D. H Lee, B. Hoffmann, J. Kressler, and G. Stöppelmann. 2001. “Influence of nanofillers on the deformation process in layered silicate/polyamide-12 nanocomposites.” *Polymer* 42:1095–1100.
- Kim, J., T. Oh, and D. Lee. 2003. “Preparation and characteristics of nitrile rubber (NBR) nanocomposites based on organophilic layered clay.” *Polymer International* 52:1058–1063.
- Kissinger, H. E. 1957. “Reaction kinetics in differential thermal analysis.” *Analytical chemistry* 29:1702–1706.
- Lee, C., X. Wei, J. W Kysar, and J. Hone. 2008. “Measurement of the elastic properties and intrinsic strength of monolayer graphene.” *Science* 321:385.
- Lopez-Manchado, M. A., M. Arroyo, B. Herrero, and J. Biagiotti. 2003. “Vulcanization kinetics of natural rubber-organoclay nanocomposites.” *Journal of Applied Polymer Science* 89:1–15.
- Lotya, M. et al. 2009. “Liquid phase production of graphene by exfoliation of graphite in surfactant/water solutions.” *J. Am. Chem. Soc* 131:3611–3620.
- Maiti, M., S. Mitra, and A. K Bhowmick. 2008. “Effect of nanoclays on high and low temperature degradation of fluoroelastomers.” *Polymer Degradation and Stability* 93:188–200.
- McAllister, M. J et al. 2007. “Single sheet functionalized graphene by oxidation and thermal expansion of graphite.” *Chem. Mater* 19:4396–4404.
- Menard, K. P. 2008. *Dynamic mechanical analysis: a practical introduction*. CRC.

- Novoselov, K. S. et al. 2004. "Electric field effect in atomically thin carbon films." *Science* 306:666.
- Paciorek, K. L., L. C. Mitchell, and C. T. Lenk. 2003. "Mechanism of amine crosslinking of fluoroelastomers. I. Solution studies." *Journal of Polymer Science* 45:405–413.
- Ramanathan, T. et al. 2008. "Functionalized graphene sheets for polymer nanocomposites." *Nature Nanotechnology* 3:327–331.
- Rong, M. Z et al. 2001. "Structure-property relationships of irradiation grafted nano-inorganic particle filled polypropylene composites." *Polymer* 42:167–183.
- Rozman, H. D. et al. 2001. "THE EFFECT OF OIL EXTRACTION OF THE OIL PALM EMPTY FRUIT BUNCH ON THE MECHANICAL PROPERTIES OF POLYPROPYLENE–OIL PALM EMPTY FRUIT BUNCH–GLASS FIBRE HYBRID COMPOSITES." *Polymer-Plastics Technology and Engineering* 40:103–115.
- Schniepp, H. C et al. 2006. "Functionalized single graphene sheets derived from splitting graphite oxide." *J. Phys. Chem. B* 110:8535–8539.
- Shimazaki, Y. et al. 2007. "Excellent thermal conductivity of transparent cellulose nanofiber/epoxy resin nanocomposites." *Biomacromolecules* 8:2976–2978.
- Sternstein, S. S., and A. J Zhu. 2002. "Reinforcement mechanism of nanofilled polymer melts as elucidated by nonlinear viscoelastic behavior." *Macromolecules* 35:7262–7273.
- Thomassin, J. M et al. 2006. "Improvement of the barrier properties of Nafion® by fluoro-modified montmorillonite." *Solid state ionics* 177:1137–1144.
- Valentini, L., J. Biagiotti, J. M. Kenny, and M. A.L Machado. 2003. "Physical and mechanical behavior of single-walled carbon nanotube/polypropylene/ethylene-propylene-diene rubber nanocomposites." *Journal of Applied Polymer Science* 89:2657–2663.
- Wang, Y., L. Liu, Y. Luo, and D. Jia. 2009. "Aging behavior and thermal degradation of fluoroelastomer reactive blends with poly-phenol hydroxy EPDM." *Polymer Degradation and Stability* 94:443–449.
- Xie, W. et al. 2001. "Thermal degradation chemistry of alkyl quaternary ammonium montmorillonite." *Chem. Mater* 13:2979–2990.
- Yang, F., Y. Ou, and Z. Yu. 1998. "Polyamide 6/silica nanocomposites prepared by in situ polymerization." *Journal of Applied Polymer Science* 69:355–361.

- Yang, I. K, and P. H Tsai. 2007. "Preparation and characterization of polyether-block-amide copolymer/clay nanocomposites." *Polymer Engineering and Science* 47:235–243.
- Zeng, C., and L. J Lee. 2001. "Poly (methyl methacrylate) and polystyrene/clay nanocomposites prepared by in-situ polymerization." *Macromolecules* 34:4098–4103.
- Zou, H., S. Wu, and J. Shen. 2008. "Polymer/silica nanocomposites: preparation, characterization, properties, and applications." *Chem. Rev* 108:3893–3957.

CHAPTER 3

PREPARATION AND PROPERTIES OF FLUOROTHERMOPLASTIC ELASTOMER NANOCOMPOSITES PROCESSED THROUGH DYNAMIC VULCANIZATION

3.1 Abstract

In this chapter, a novel type of fluorothermoplastic elastomer (F-TPE) nanocomposites, were prepared by dynamic vulcanization method. A fluoroelastomer and a fluorothermoplastic were blended using a Haake torque rheometer. The fluoroelastomer was partially vulcanized during blending and was cured further in a subsequent post cure process. While the elastomer imparted the preferred elastic properties to the blend, the fluorothermoplastic made the blend melt processable and reprocessable. Nanoclay, nano silica and expanded graphite were added to the blends and their effects on mechanical, dynamic, and thermal properties of the blends were studied. Tensile properties of the mechanical properties of the F-TPE were studied. Glass transition and viscoelastic behavior of the nanocomposites were characterized by dynamic mechanical analysis (DMA). Thermal stability of the nanocomposites was evaluated by thermal gravimetric analysis (TGA). Scanning electron microscopy (SEM) and transmission electron microscopy (TEM) were used to study the distribution of the nanofillers and phase structure of the composites. It was found that all the nanofillers could increase the mechanical properties and storage modulus of the F-TPE blends. Thermal stability of the

blends was influenced differently depending on the nanofiller type. The nanofillers appeared to preferentially reside in the elastomer phase of the blends.

3.2 Introduction

Thermoplastic elastomers (TPE) have attracted much attention because they combine the processing characteristics of thermoplastic and the elastomeric characteristics of rubbers in one material (Ellul, et al. 2004; Sirisinha, et al. 2004; Ma et al. 2004). International Institute of Synthetic Rubber Producers defines TPE as “polymers, polymer blends or compounds which, above their melt temperatures, exhibit thermoplastic character that enables them to be shaped into fabricated articles and which, within their design temperature range, possess elastomeric behavior without crosslinking during fabrication. This process is reversible and the products can be reprocessed and remoulded.” (Brydson 1995). Therefore, they show rubber elasticity at service temperatures but can be thermoplastically processed at elevated temperatures. TPE becomes an attractive material also due to the possibility of changing material properties, such as tensile properties, through varying the ratio of plastic/ elastomer fractions (Weidisch et al. 2001).

Most TPEs are basically phase-separated systems and usually one phase is rigid at ambient temperature whereas the other is rubbery. The rigid phase gives these TPEs strength, without which the elastomer phase would be easy to deform under stress and on the other hand, the elastomer phase provides flexibility and elasticity to the system (Drobny 2007). Because phase separation could influence the mechanical properties of polymer blends, it is critical to investigate the microstructure and morphology of TPEs.

For example, in poly-(styrene-*b*-butadiene-*b*-styrene) (SBS) triblock copolymers, polystyrene micro domains dispersed in the continuous rubbery poly(butadiene) matrix. Mechanical properties of the polymer could be controlled by changing the ratio of the styrene to butadiene blocks (Rader, 1996). Weidisch et al. (2001) showed that in the polystyrene(PS)-polyimide(PI) multigraft copolymer, the number of PS branch points on the PI backbone played a determining role in the morphology and mechanical properties of the copolymer. To study the phase morphology of TPE, nuclear magnetic resonance (NMR) (Powers et al. 2008), scanning electron microscopy (SEM) (Cheng et al. 2008) and transmission electron microscopy (TEM) (Zhu et al. 2006) are usually used..

Fluorothermoplastic elastomers (F-TPE), sometimes also referred to as fluorinated thermoplastic rubbers, are a class of fluorocopolymers or a physical mix of fluoropolymers (usually a plastic and a rubber) which combines the properties of a fluorothermoplastic and a fluoroelastomer. Generally, these types of materials show the following advantages: (1) advantages typical of both rubbery materials and plastic materials, (2) processable and recyclable like thermoplastic, (3) great properties improvement achieved by small amount reinforced nanofillers. While the advantages of TPE lead to extensive applications, the limitations are also obvious: high cost of raw materials and higher temperature sensitivity than competitive elastomer. For example, Acquarula et al. (1999) showed that the crosslinking method of copolyamide-containing TPE had a significant effect upon elevated temperature performance.

To obtain high performance F-TPE, the material is often generated by dynamic vulcanization, a process of vulcanizing the elastomer during its melt-mixing with a non-vulcanizing thermoplastic polymer (Holden, et al. 2004). In contrast, static vulcanization

would lead to a 3-D cross-linked network throughout a single phase elastomer material, which makes material reprocessing impossible (Li et al. 2006). During dynamic vulcanization, the morphology and compatibility of TPE blends varies depending on the content of the dispersed elastomer and the compatibilizer used, which in turn leads to wide variation in mechanical properties of the resulting composites. It is accepted that for an immiscible binary blend two separate glass transitions (corresponding to the two components) can be observed and for a miscible blend only one glass transition is observed (Mader et al. 1999).

Though many studies on TPEs have been carried out, the influence of nanofillers on mechanical and thermal properties of high performance TPE systems, e.g., fluorothermoplastic elastomer needs to be further investigated. It has also been found that many TPEs, e.g. diene rubber- polyolefin based thermoplastic elastomer (Fischer 1985), butyl rubber-polypropylene based thermoplastic elastomer (Liao et al. 1994), and acrylic rubber-poly(vinylidene fluoride) based thermoplastic elastomer (Li et al. 2006), show higher mechanical properties through dynamic vulcanization. However, few studies on dynamic vulcanization of F-TPE have been reported. Further, the effects of nanofillers on F-TPE dynamic vulcanization and on the properties of the resulting F-TPE nanocomposites also deserve an in-depth investigation because of the significant effects of nanofillers on the vulcanization and properties of fluoroelastomers.

In this chapter, F-TPE nanocomposites with different types and contents of nanofillers were prepared by dynamic vulcanization process. The properties of the nanocomposites including thermal, mechanical, and dynamic properties were investigated. The objectives of this research include:

- (1) preparing novel F-TPE and F-TPE nanocomposites through dynamic vulcanization;
- (2) investigating the dispersion of nanofillers and the phase morphology of F-TPE nanocomposites
- (3) evaluating the effects of the nanofillers on the properties of F-TPE.

3.3 Experimental

3.3.1 Materials

Fluoroelastomer vinylidene fluoride-hexafluoropropylene (VDF-HFP, FC-2260) and fluorothermoplastic hexafluoropropylene-tetrafluoroethylene (HFP-TFE, FEP-6322) were kindly supplied by Dyneon LLC. 2, 5-dimethyl-2, 5-di (t-butylperoxy)-hexane (DBPH-50), an organic peroxide used as the fluoroelastomer crosslinking agent, was obtained from R.T. Vanderbilt Company, Inc. Commercial organically modified nanoclay I.34TCN (hereafter “S-clay”) was purchased from Nanocor Inc. According to literature, this organo-nanoclay is prepared by treating original montmorillonite clay with a quaternary ammonium salt type cationic surfactant. The ammonium salt has two alkyl (tallow) tails and hydroxyl group attached to either the tallow tail or the ammonium head (Yang and Tsai 2007). Silicon dioxide nanoparticle (~10 nm) was purchased from Sigma-Aldrich, and graphite from Fisher Scientific. In addition, we also prepared the fluoroaliphatic quaternary ammonium fluorosurfactant (FS-1620, DuPont) treated nanoclay (designated as “FS-clay”) following the method in the literature (Thomassin et al. 2006). 3-aminopropyltriethoxysilane, a silane coupling agent used to treat silica was

purchase from Acros Organics. The procedures for graphite and silica surface treatments have been detailed in Chapter 2.

3.3.2 Preparations

Dynamic vulcanization of F-TPE was performed using a Haake torque rheometer (Haake Rheomix 600). The ratio of fluorothermoplastic/fluoroelastomer was 60/40 for all F-TPE blends. Different contents of nanofillers were added to the blends during mixing. The entire processing procedure could be divided into the following three steps: (1) 30.8 grams of the elastomer together with 2.5% curing agent (DBPH-50) were mixed in the rheometer for 3min at 177 °C; (2) 46.24 grams of thermoplastic were added into the rheometer, the mixing temperature was increased to 255 °C, and the mixing continued for 5 minutes until the thermoplastic was fully molten; (3) different contents of nanofillers based on the total weight of the plastic and elastomer were added into the rheometer and mixed for another 12 minutes. The rotation speed of the rheometer rotors was maintained at 80 rpm during the whole process.

After blending, the material was removed from the rheometer and pressed into sheets (1.5 mm × 40mm × 40mm) at 242°C using a compression mold and a hot press machine (Model 3851-0, Carver Inc.). The temperature and pressure were maintained for 24 hr to make sure the fluoroelastomer was fully cured. The obtained sheets were used for further characterizations. The formulations of all the prepared F-TPE nanocomposites have been listed in Table 3.1.

Table 3.1 Formulations of neat F-TPE and F-TPE nanocomposites

Formulations	Composition
Neat F-TPE	FC 2260 + FEP 6322 ^a + 2.5% Curing Agent ^b
F-TPE/ 2% S-clay	FC 2260 + FEP 6322 + 2.5% Curing Agent + 2% S-clay ^c
F-TPE/ 2% FS-clay	FC 2260 + FEP 6322 + 2.5% Curing Agent + 2% FS-clay
F-TPE/ 2% T-G	FC 2260 + FEP 6322 + 2.5% Curing Agent + 2% treated graphite
F-TPE/ 4% T-G	FC 2260 + FEP 6322 + 2.5% Curing Agent + 4% treated graphite
F-TPE/ 2% UT-SiO ₂	FC 2260 + FEP 6322 + 2.5% Curing Agent + 2% untreated silica
F-TPE/ 4% UT-SiO ₂	FC 2260 + FEP 6322 + 2.5% Curing Agent + 4% untreated silica
F-TPE/ 2% T-SiO ₂	FC 2260 + FEP 6322 + 2.5% Curing Agent + 2% treated silica
F-TPE/ 4% T-SiO ₂	FC 2260 + FEP 6322 + 2.5% Curing Agent + 4% treated silica

a. the ratio of plastic/ elastomer was 60/40 (weight / weight).

b. curing agent content was based on the total weight of plastic and elastomer.

c. nanofiller content was based on the total weight of plastic and elastomer

(excluding the curing agent)

3.3.3 Characterizations

Dynamic mechanical analysis (DMA) was carried out on a DMA Q800 dynamic mechanical analyzer (TA instruments) using a single cantilever configuration. DMA samples measuring 17.5mm ×15mm ×1.5mm were cut from the pressed sheets. All samples were tested from -60 to 120 °C at a ramp rate of 3 °C/min and a frequency of 1 Hz. The oscillating strain for all the samples was 0.02%. The storage modulus and tanδ of the samples were recorded as a function of the temperature.

Thermogravimetric analysis (TGA) was performed on a SDT Q600 thermogravimetric analyzer (TA instruments). F-TPE samples (ca. 10 mg) were scanned

from 30 to 800 °C under continuous nitrogen flow at a heating rate of 20 °C/min. The temperature corresponding to the maximum weight loss rate was considered as the sample degradation temperature (T_{\max}).

For tensile test, dumbbell-shaped specimens were cut from the compressed sheets using a Type IV (ASTM D638) sample cutter and tested according to ASTM D 638–91. Five replicates for each formulation were tested using an Instron 4466 (capacity 500 N) at a tensile rate of 2 mm/min. Tensile strain were monitored by an EIR laser extensometer (model LE-05).

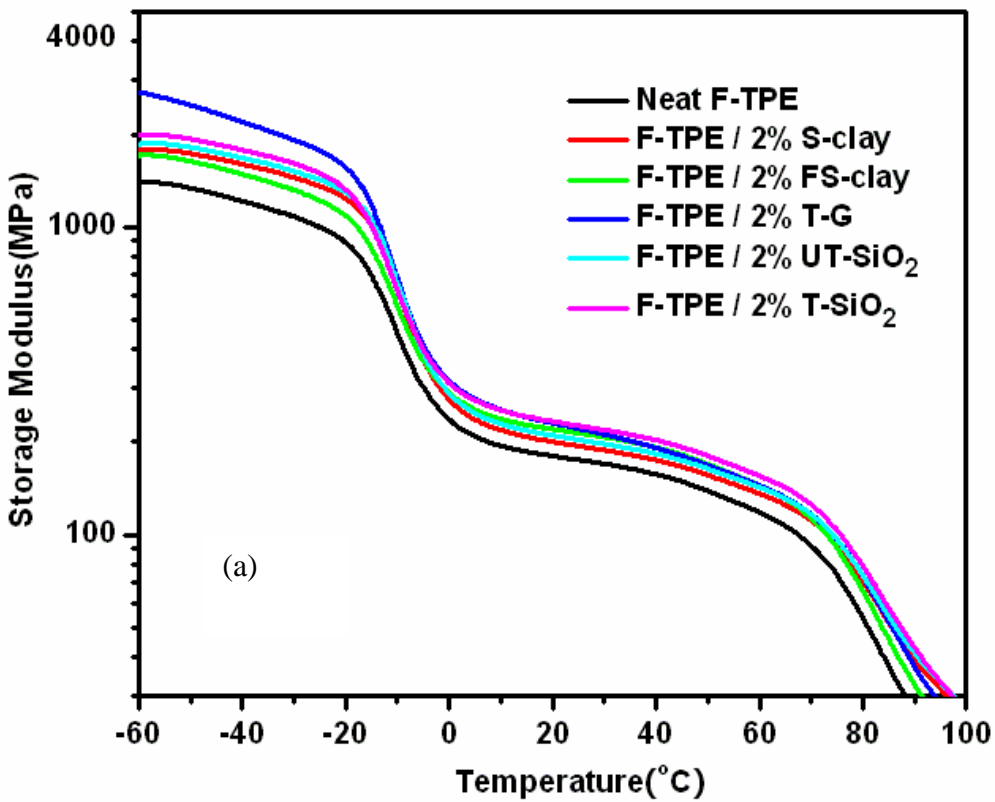
F-TPE morphology and nanofiller dispersion were studied by a transmission electron microscope (TEM) (JEOL 1200EX) operating at 100 kV. Sample slices (80-100 nm thick) were cut using an ultramicrotome (Powertome X, Boeckeler Instrument) at -50 °C. The slices floated in alcohol and were collected using copper grids. Field emission scanning electron microscopy (FE SEM, Quanta 200F) was also used to investigate the cryo-sliced and cryo-fractured surfaces of the samples.

3.4 Results and Discussion

3.4.1 Dynamic Mechanical Properties

The dynamic mechanical properties of the F-TPE blends as a function of temperature and nanofiller type were examined by DMA measurements. Figure 3.1 compares the storage modulus and $\tan\delta$ of the samples containing 2% different nanofillers. Two modulus precipitations on each curve were evident, with the one at ca. -10°C corresponding to the glass transition of the elastomer component in the blends and the one at ca. 85 °C to the thermoplastic component. Compared to the modulus of the neat

fluoroelastomer (Figure 2.4 of Chapter 2), the modulus of neat F-TPE (without any nanofillers) was much higher (ca. 200 vs 20MPa) due to the incorporation of the fluorothermoplastic to the elastomer. Figure 3.1(a) also shows that neat F-TPE had the lowest storage modulus among all the samples and the addition of 2% nanofillers increased the modulus over the whole range of testing temperatures. The modulus increase was larger at the temperatures below the fluoroelastomer T_g than at the temperatures above.



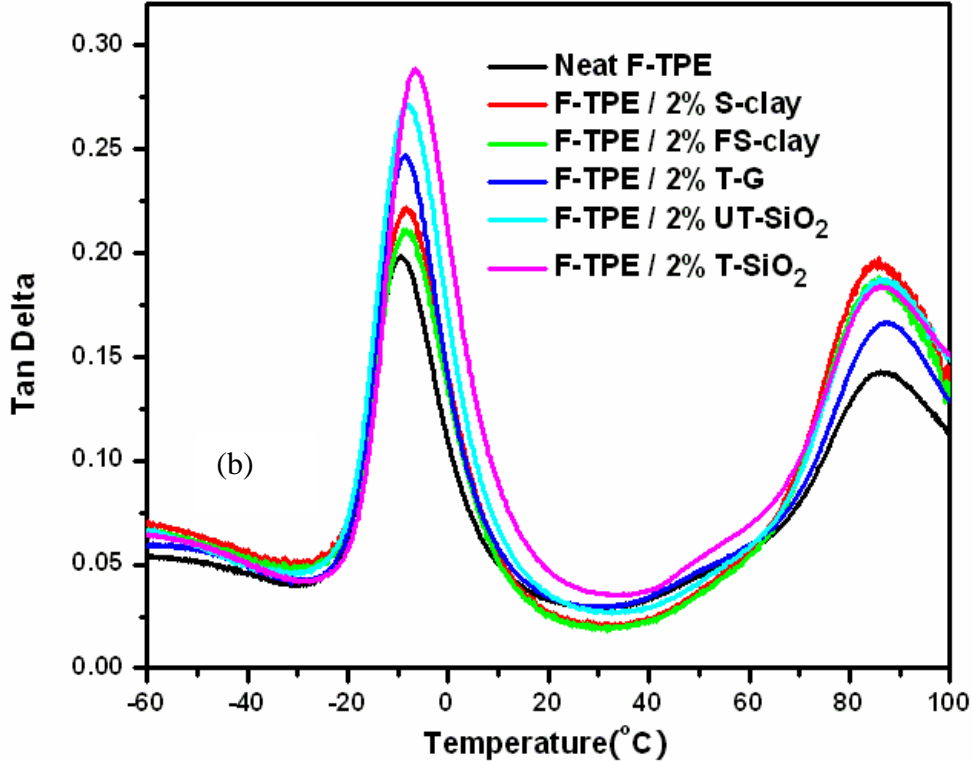


Figure 3.1 Storage modulus (a) and $\tan\delta$ (b) curves of neat F-TPE and F-TPE nanocomposites comprising 2% of different nanofillers.

Figure 3.1(b) compares $\tan\delta$ curves of the same set of samples. It shows two distinctive relaxation peaks at -9.5 and 85.4 °C (for the neat F-TPE), corresponding to the glass transitions of the elastomer and thermoplastic components, respectively. Generally, at 2 wt% nanofiller content, all the fillers show negligible effects on the glass transition temperature of the thermoplastic component. FS-clay, S-clay, and UT-SiO₂ led to small increases in the T_g of the elastomer component (ca. 1 °C) (see also Table 3.2). In contrast, T-SiO₂ increased the T_g by 2.5 °C. This result was consistent with the results of the fluoroelastomer composites (Chapter 2) in which T-SiO₂ also caused the largest increase

in the T_g of elastomer. The breadth of the glass transition peaks of the elastomer also increased after the addition of the nanofillers, whereas the breadth of the thermoplastic remained largely unchanged. The reason for apparent increase in the T_g of the elastomer phase rather than the thermoplastic phase was probably due to the nanofillers' preferential distribution in the elastomer phase, which was confirmed by the TEM and SEM analysis of morphology of the composites. The distributed nanofillers hinder the chain mobility of the elastomer through their interactions with the polymer, leading to higher T_g and larger peak breadth (due to relaxation heterogeneity).

At 4 wt% nanofiller content, UT-SiO₂ and T-SiO₂ increase the T_g of the elastomer by 3.6 and 5°C, respectively, whereas all the fillers increase the T_g of the thermoplastic by ca. 2°C (Figure 3.2b and Table 3.2). This could be due to the migration of the nanofillers to the thermoplastic phase at high filler content. Compared to the samples containing 2% nanofillers, F-TPE nanocomposites containing 4 wt% nanofillers also resulted in much higher storage modulus over the whole temperature range (Figure 3.2a). Among all the used nanofillers, T-SiO₂ results in the largest increase in both T_g and storage modulus (second highest at the temperatures above the elastomer T_g) due to its chemical bonding with the elastomer and its crosslinking agent function.

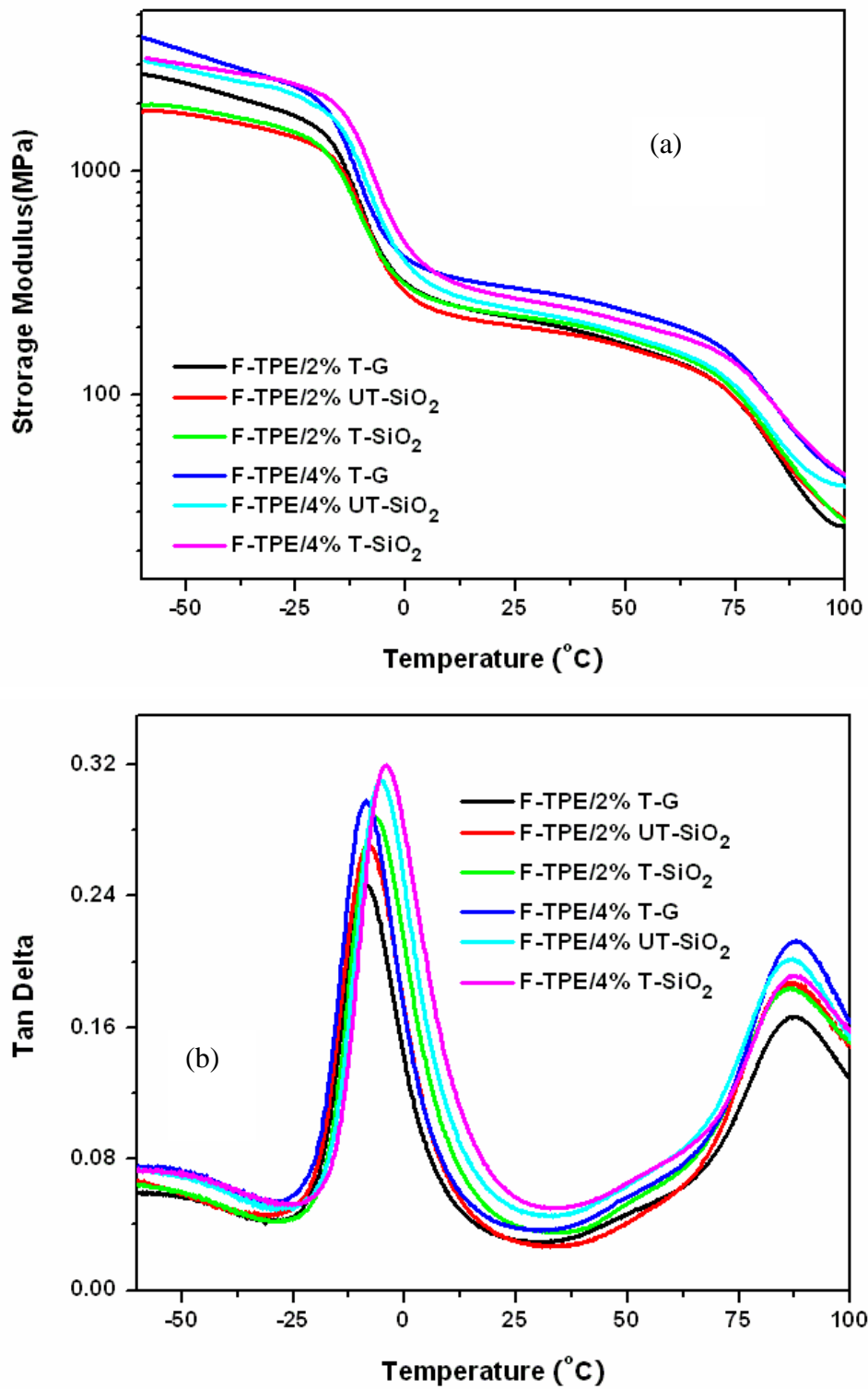


Figure 3.2 Comparison of the storage modulus (a) and $\tan\delta$ (b) of F-TPE nanocomposites comprising 4% of different nanofillers. The modulus and $\tan\delta$ of F-TPE-2% T-SiO₂ were also given for comparison.

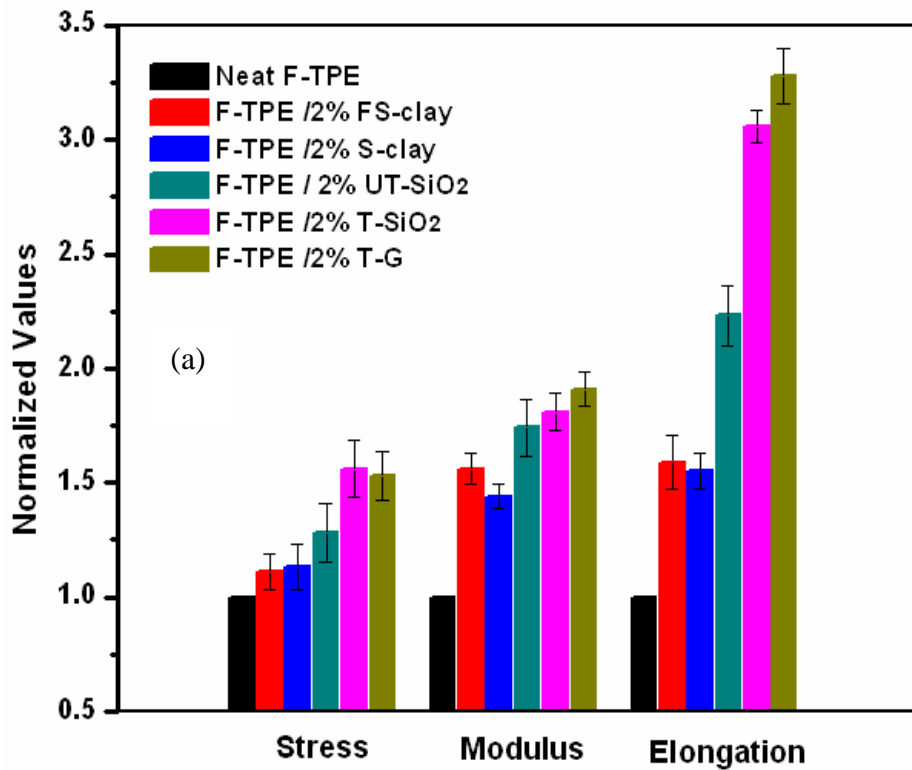
Table 3.2 Thermal analysis results of neat F-TPE and F-TPE nanocomposites

Formulations	Elastomer Tg (°C)	Plastic Tg (°C)	T _{max} of Elastomer (°C)	T _{max} of Plastic (°C)
Neat F-TPE	-9.1	85.4	474.5	575.2
F-TPE/ 2% S-clay	-8.2	85.3	470.2	571.4
F-TPE/ 2% FS-clay	-8.0	85.6	465.6	568.8
F-TPE/ 2% T-G	-8.8	84.9	498.2	581.3
F-TPE/ 2% UT-SiO ₂	-8.0	85.8	501.4	572.5
F-TPE/ 2% T-SiO ₂	-6.6	86.5	505.3	576.0
F-TPE/ 4% T-G	-8.6	87.9	504.5	576.8
F-TPE/ 4% UT-SiO ₂	-5.5	87.1	502.3	580.9
F-TPE/ 4% T-SiO ₂	-4.1	87.1	510.2	576.4

3.4.2 Tensile Properties

Figure 3.3 compares the tensile strength, modulus, and elongation of neat F-TPE and the F-TPE nanocomposites comprising different types and contents of nanofillers. The neat F-TPE exhibits a tensile strength, modulus, and elongation of 8.5 MPa, 152.3MPa, and 12.2%, respectively. The addition of 2% nanofillers significantly increases all three properties. Among all the used nanofillers, FS-clay and S-clay displayed the lowest degree of property improvement. T- SiO₂ and T-G were the two nanofillers that show the most significant reinforcing and toughening effects. By including 2% T-SiO₂ or T-G, the strength, modulus, and elongation of the composites were ca. 1.5, 1.8, and 3.2 times of that of the neat F-TPE. The improvement in tensile strength and modulus indicates homogeneous dispersion of the nanofillers and strong interfacial bonding between the fillers and the polymer matrix. T-SiO₂ can form covalent crosslinks with the fluoroelastomer and therefore the large improvement is expected for T-SiO₂. However,

DMA results showed that T-G was not able to increase the T_g of the elastomer, an indication of poor interaction between the two phases. The tensile properties of the fluoroelastomer nanocomposites (Figure 2.6 in Chapter 2) also indicate that T-G induced smaller property improvement than T-SiO₂. The significant property improvement of the F-TPE composites by the addition of T-G may be attributed to its good distribution in the composites or interaction with the thermoplastic phase of the composites, which requires further in-depth study on the morphology of the composites.



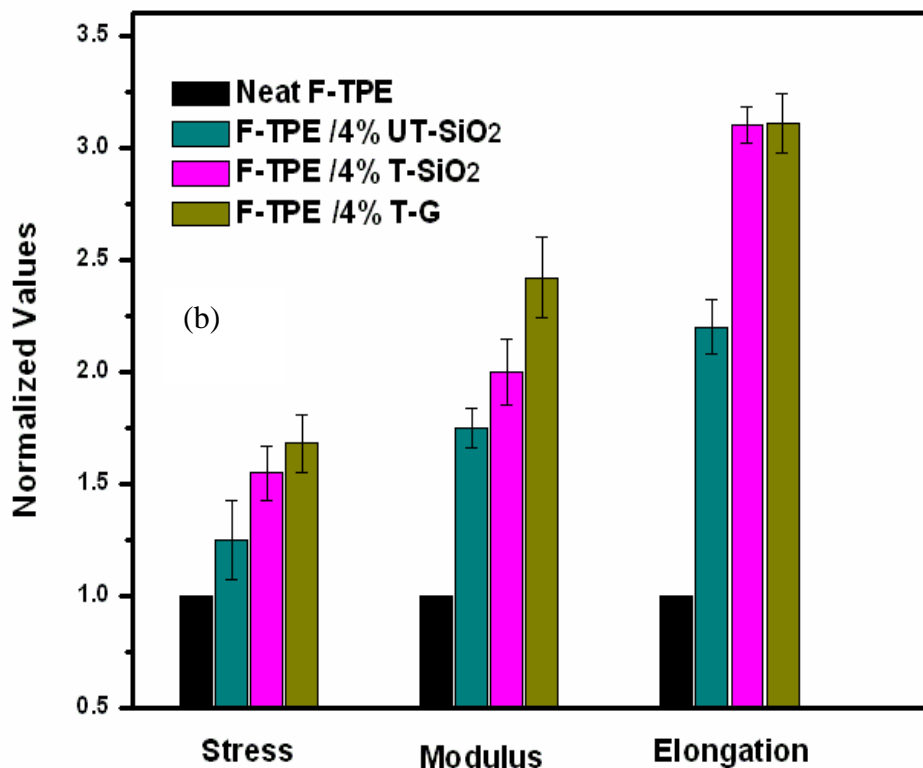


Figure 3.3 Tensile properties of F-TPE nanocomposites comprising 2% (a) and 4% (b) of different nanofillers.

All the nanofillers led to significant enhancement in sample elongation, especially T- SiO₂ and T-G. Nanoparticles have been shown to be able to toughen polymers (Jiang, et al. 2007). The mechanism of toughening is believed to be debonding induced stress state change (plane strain to plane stress) which allows extensive plastic deformation in the samples. Microstructure of the fractured surfaces of the tested samples is required to identify the toughening mechanism of the nanofillers on the F-PTE systems.

Tensile properties of the F-TPE blends containing 4% UT-SiO₂, T-SiO₂, and T-G are compared in Figure 3.3(b). Increasing UT-SiO₂ and T-SiO₂ content from 2 to 4% only resulted in slightly further improvement in strength and modulus. Only the strength and modulus of the composites containing T-G continuously increased with filler concentration, which imparted the F-TPE /4% T-G composite the highest strength and modulus among all the tested composites.

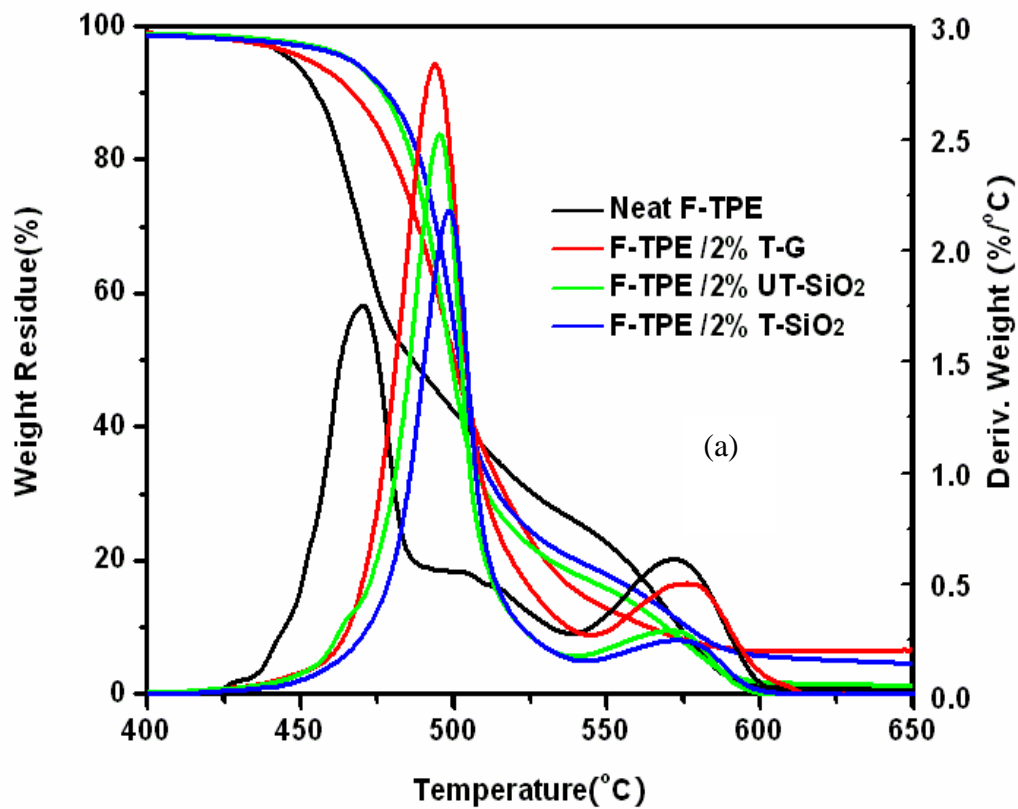
The different reinforcing behaviors between UT-SiO₂ /T-SiO₂ and T-G at the two filler concentrations imply that the nanofillers reinforced the F-TPE blend through different ways. T-SiO₂ displayed the highest reinforcing effect in fluoroelastomer composites (Figure 2.7, Chapter 2) due to its strong interfacial bonding with the elastomer and its crosslinking function to the elastomer. It is not anticipated that T-SiO₂ will be similarly effective in reinforcing the thermoplastic phase in the F-TPE blend because there is no special interactions between them. Therefore, in the F-TPE blend only the elastomer phase was effectively reinforced by T-SiO₂. In comparison, although T-G did not reinforce the elastomer to the same degree as T-SiO₂ did (Figure 2.7, Chapter 2) due to its lack of chemical reaction to the elastomer, it might reinforce the thermoplastic phase better than does T-SiO₂ because of its favorable shape. When the T-G content in the composites increased from 2 to 4%, more T-G particulates were distributed in the thermoplastic phase compared to at 2% content. Therefore, the thermoplastic phase, which was the major component of the F-TPE blend, was reinforced to a higher degree. As a result, the overall reinforcing effect of T-G can be higher than that of T-SiO₂, which led to the highest properties of the blend.

3.4.3 Thermal Stability

In Chapter 2 we have shown that untreated/ treated silica and treated graphite can increase the thermal degradation onset temperature of FC2260. The effects of these fillers on the thermal stability of the F-TPE blends are compared in Figure 3.4 (a) and (b) and the results are summarized in Table 3.2.

Neat F-TPE demonstrated a two stage thermal degradation behavior, originating from the degradation of the elastomer phase (low temperature) and the thermoplastic phase (high temperature), respectively. The temperature at which the maximum degradation rate takes place is designated as T_{\max} and can be obtained from the peak temperature of the derivative weight loss curve. By incorporating 2% T-G, UT-SiO₂ and T-SiO₂, the T_{\max} of the elastomer phase increased from 474.5 to 498.2, 501.4 and 505.3°C, respectively (Table 2). By adding 4% T-G, UT- SiO₂ and T- SiO₂, T_{\max} further increased to 504.5, 502.3, and 510.2°C, respectively. Among the tested nanofillers, T-SiO₂ led to the largest increase in T_{\max} of the elastomer phase. The same phenomenon was observed in the FKM composites (see Chapter 2). On the other hand, FS-clay and S-clay decreased the T_{\max} of the elastomer phase, due to the decomposition of the surfactant used for clay treatment. Without nanofillers, the T_{\max} of the elastomer phase in the pure F-TPE was remarkably lower than that of the pure FKM (474.5 compared to 492.4°C). After adding the nanofillers (e.g. T-G, UT- SiO₂, or T- SiO₂), the T_{\max} of the elastomer phase was increased to even higher than that of the FKM nanocomposites (Table 3.2). In other words, the nanofillers showed stronger effect on increasing the T_{\max} of the elastomer in F-TPE than in FKM (ca. 30 compared to 10 °C). The reason for this phenomenon is not clear yet.

The T_{max} of the thermoplastic phase in the pure F-TPE is 575.2°C, almost 100°C higher than that of the elastomer phase (Table 3.2). In general, the effect of the nanofillers on the T_{max} of the thermoplastic phase is much smaller compared to that of the elastomer phase. A possible reason is due to the nanofiller's preferential distribution in the elastomer phase.



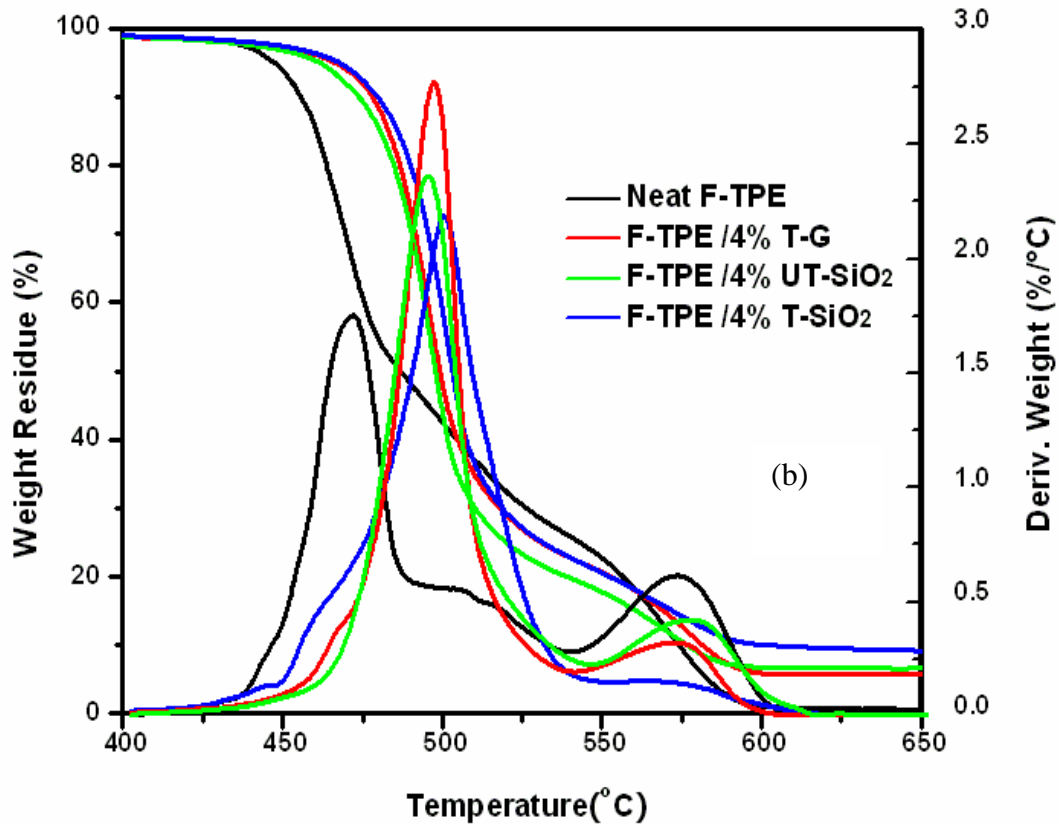
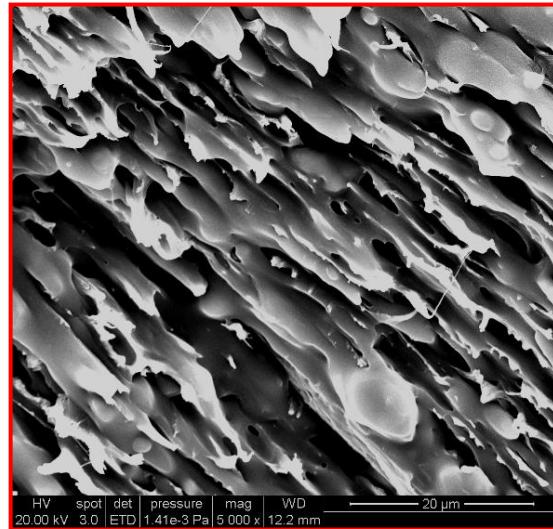
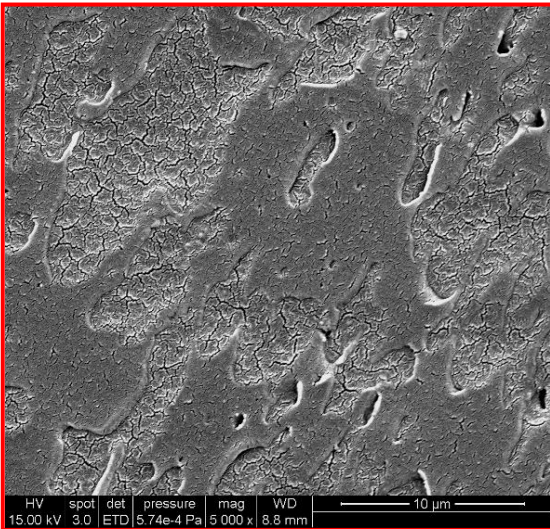
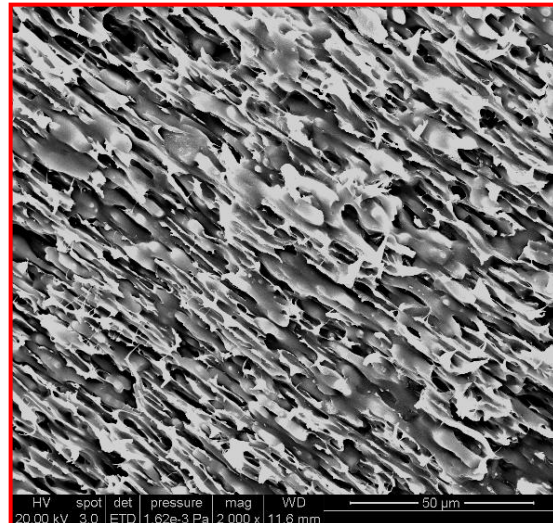
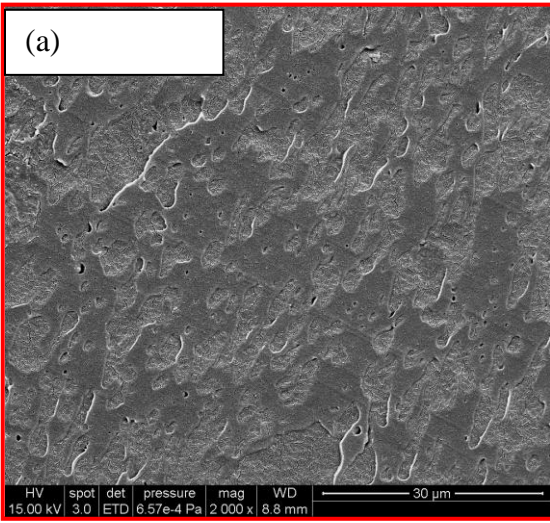


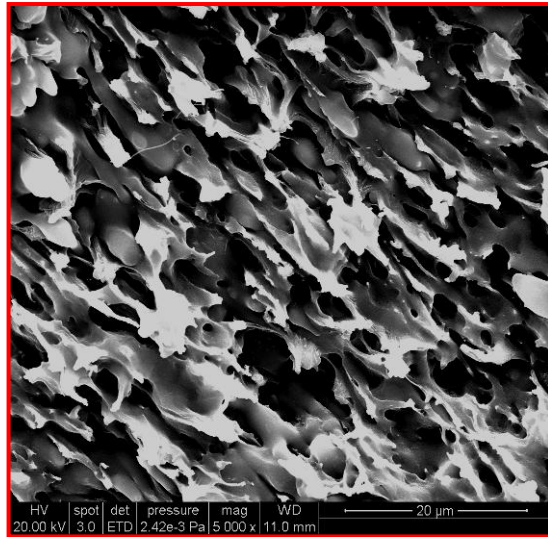
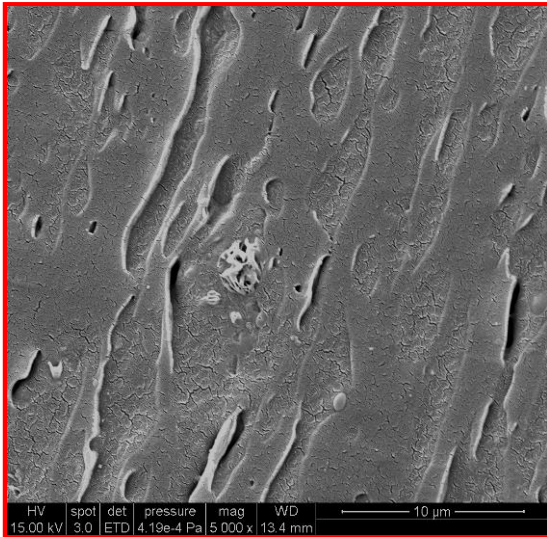
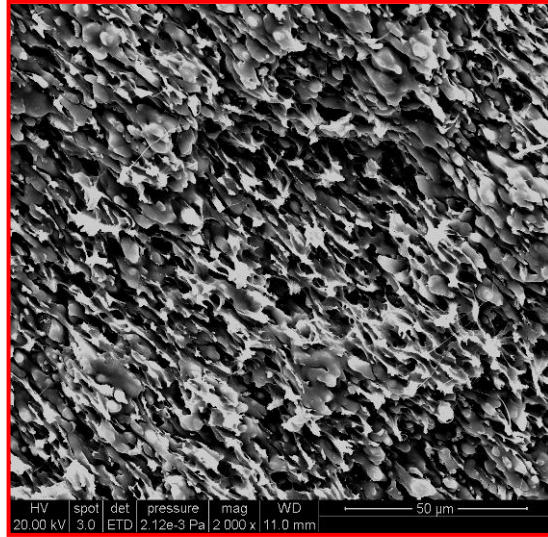
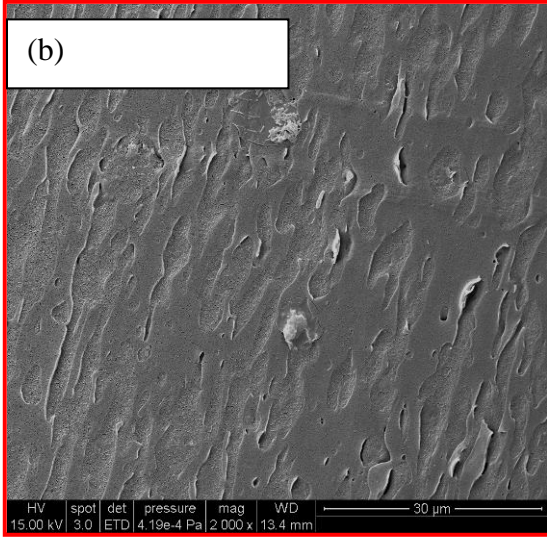
Figure 3.4 Thermal stability of neat F-TPE and F-TPE nanocomposites: (a) 2% nanofiller content; (b) 4% nanofiller content.

3.4.4 Dispersion and Morphology

It is understood that state of filler dispersion in the polymer matrix not only greatly influence the mechanical properties (e.g. tensile stress, modulus) of the polymer composites (Zhang et al. 2006) but also the heat capacity and crystallization (Wurm et al. 2010). In order to better understand how the nanofillers dispersed in the multi-phase F-TPE blends as well as their influence on the morphology of the system, SEM and TEM analysis were carried out and the micrographs were presented in Figure 3.5, Figure 3.6 and Figure 3.7.

Both cryo-fractured and cryo-sliced surfaces of the neat F-TPE, F-TPE/ T-SiO₂ and F-TPE/ UT-SiO₂ composites were prepared for SEM observations and the results were shown in Figure 3.5. From the cryo-sliced surfaces, a two phase structure is evident for all the samples. The sunken areas in the micrographs were the crosslinked rubber phase and the other areas are the thermoplastic phase. Both the cryo-sliced surfaces and the cryo-fractured surfaces show co-continuous phase structures for neat F-TPE, F-TPE/ T-SiO₂ and F-TPE/ UT-SiO₂ composites. Figure 3.6 compares the cryo-sliced surface of neat F-TPE, F-TPE/ T-SiO₂, F-TPE/ UT-SiO₂, and F-TPE/ T-G. It appears that the F-TPE/T-G composite has the strongest interfacial bonding. The two phases in this composite are tightly “fused”, which makes its two-phase structure the least discernable one among the four samples. This may attribute to the highest tensile properties of the F-TPE/T-G nanocomposites. Figure 3.7(a) shows the SEM micrographs of the neat F-TPE and F-TPE/ T-SiO₂ composite. The micrographs suggest that T-SiO₂ is preferentially distributed in the elastomer phase. The TEM image in Figure 3.7(b) further confirms the distribution state of the T-SiO₂ particulates, where the dark band dispersed in the continuous plastic phase is elastomer phase and spherical particles are treated silica.





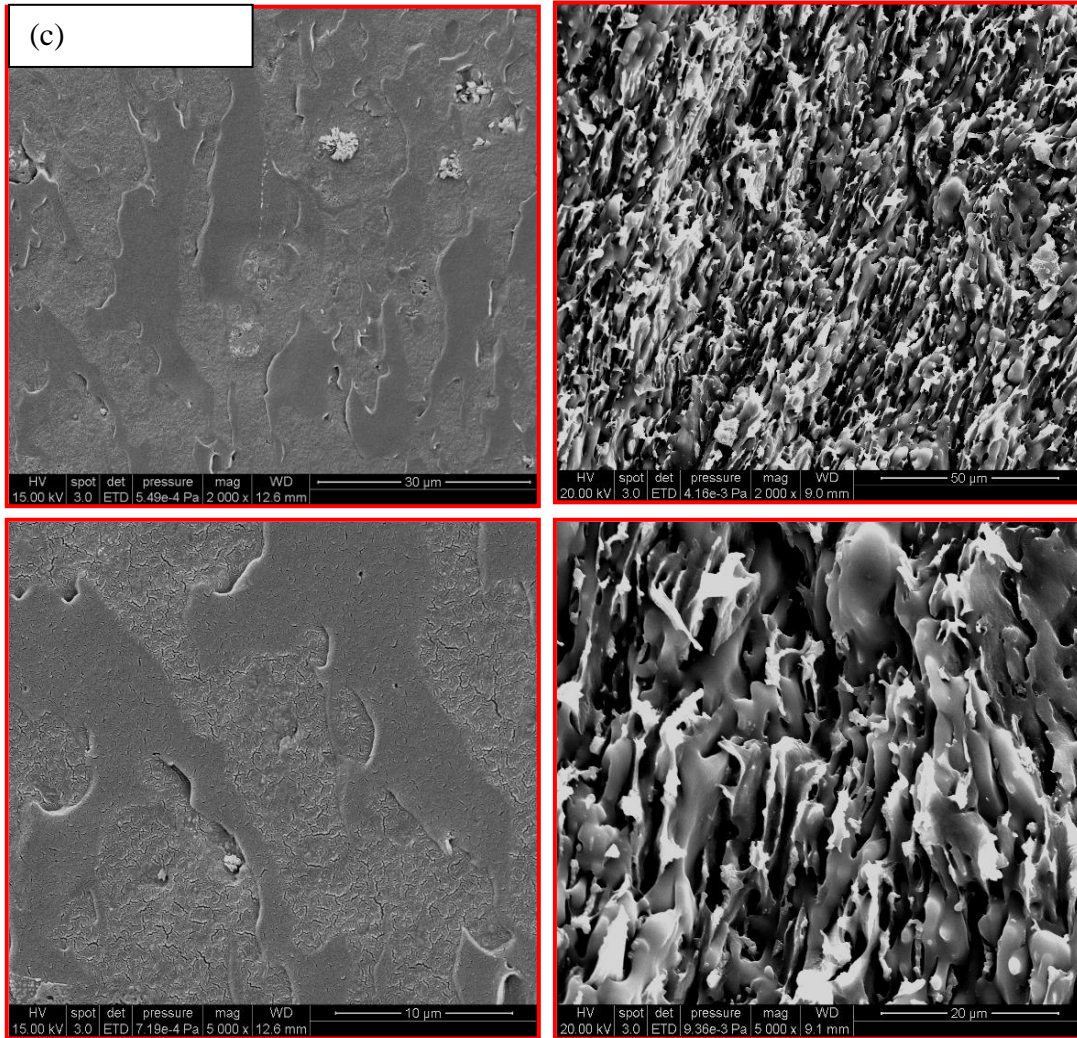


Figure 3.5 SEM images of neat F-TPE, F-TPE/ 2% UT-SiO₂ and F-TPE/ 2% T-SiO₂ formulations.

- (a) cryo-sliced (left) and cryo-fractured (right) surfaces of neat F-TPE
- (b) cryo-sliced (left) and cryo-fractured (right) surfaces of F-TPE/ 2% UT-SiO₂
- (c) cryo-sliced (left) and cryo-fractured (right) surfaces of F-TPE/ 2% T-SiO₂

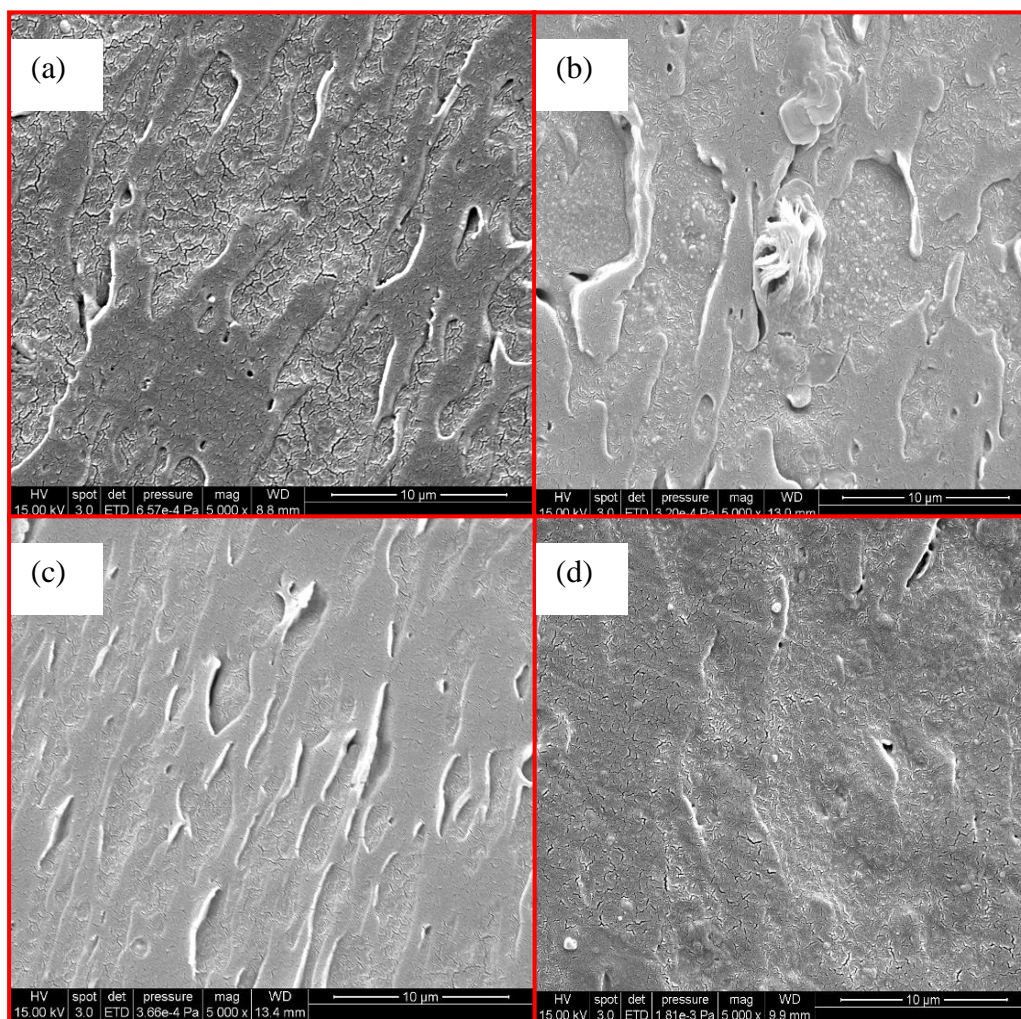


Figure 3.6 Cryo-sliced surfaces of neat F-TPE (a), F-TPE/ 2% UT-SiO₂ (b), F-TPE/ 2% T-SiO₂ (c) and F-TPE/ 2% T-G (d).

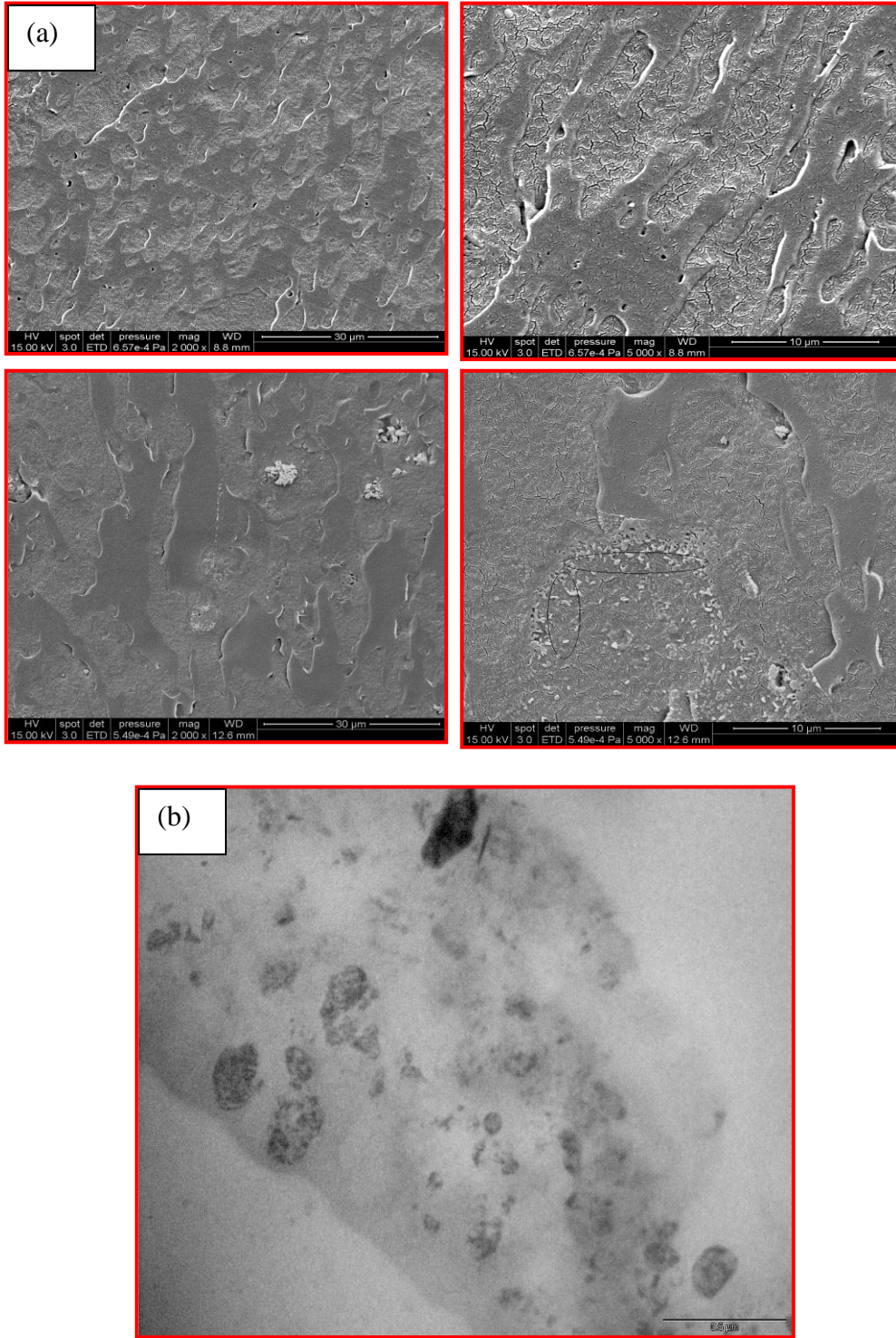


Figure 3.7 (a) SEM images of neat F-TPE (top) and F-TPE/ 2% T-SiO₂ (bottom) and (b) TEM image of F-TPE/ 2% T-SiO₂ formulation.

3.5. Conclusions

We have demonstrated that a fluorothermoplastic elastomer (F-PTE) can be prepared through a dynamic vulcanization method by using Haake rheometer mixing and compression molding. The F-PTE had the advantage of both a crosslinked elastomer and a melt processable thermoplastic. Adding different types of nanofillers to the F-PTE impart the blend remarkably different properties.

All the used nanofillers could increase tensile properties (e.g. strength, modulus, and elongation), storage modulus, and glass transition temperature of the F-PTE. The increase in the storage modulus and glass transition temperature was larger for the elastomer phase than for the thermoplastic phase due to the nanofiller's preferential distribution in the elastomer phase. In general, the higher the nanofiller content, the larger the property improvement.

Similar to its effect on FKM composites, T-SiO₂ still caused the highest increase in the glass transition temperature and degradation temperature of the elastomer phase in the F-PTE.

FS-clay and S-clay caused the degradation temperature of both the elastomer and the thermoplastic phase to decrease due to surfactant decomposition. Unlike in FKM nanocomposites, T-G, instead of T-SiO₂, resulted in the highest tensile properties of the F-PTE. This could be due to T-G's stronger reinforcing effect than T-SiO₂ on the thermoplastic phase of the F-PTE.

3.6 Reference

- Brydson, J. A. 1995. *Thermoplastic elastomers: properties and applications*. iSmithers Rapra Publishing.
- Chen, F., L. S Liu, P. H Cooke, K. B Hicks, and J. Zhang. 2008. "Performance enhancement of poly (lactic acid) and sugar beet pulp composites by improving interfacial adhesion and penetration." *Ind. Eng. Chem. Res* 47:8667–8675.
- Cheng, K. H et al. 2008. "Fabrication of and Ultraviolet Lasing in TPE/PMMA Polymer Nanowires." *The Journal of Physical Chemistry C* 112:17507–17511.
- Drobny, J. G. 2007. *Handbook of Thermoplastic Elastomers*. Plastics Design Library.
- Ellul, M. D, A. H Tsou, and W. Hu. 2004. "Crosslink densities and phase morphologies in thermoplastic vulcanizates." *Polymer* 45:3351–3358.
- Fischer, W. K. 1985. *Dynamically partially cured thermoplastic blend of monoolefin copolymer rubber and polyolefin plastic*. Google Patents.
- Holden, G., H. R Kricheldorf, and R. P Quirk. 2004. *Thermoplastic elastomers*. Hanser Verlag.
- Jiang, L., J. Zhang, and M. P Wolcott. 2007. "Comparison of polylactide/nano-sized calcium carbonate and polylactide/montmorillonite composites: Reinforcing effects and toughening mechanisms." *Polymer* 48:7632–7644.
- Li, Y. et al. 2006. "A novel thermoplastic elastomer by reaction-induced phase decomposition from a miscible polymer blend." *Macromolecules* 39:4195–4201.
- Liao, F. S, A. C Su, and T. C.J Hsu. 1994. "Damping behaviour of dynamically cured butyl rubber/polypropylene blends." *Polymer* 35:2579–2586.
- Ma, P. L, B. D Favis, M. F Champagne, M. A Huneault, and F. Tofan. 2004. "Effect of dynamic vulcanization on the microstructure and performance of polyethylene terephthalate/elastomer blends." *Polymer Engineering and Science* 42:1976–1989.
- Mader, D., M. Bruch, R. D Maier, F. Stricker, and R. Mulhaupt. 1999. "Glass transition temperature depression of elastomers blended with poly (propene) s of different stereoregularities." *Macromolecules* 32:1252–1259.
- Powers, D. S, R. A Vaia, H. Koerner, J. Serres, and P. A Mirau. 2008. "NMR characterization of low hard segment thermoplastic polyurethane/carbon nanofiber composites." *Macromolecules* 41:4290–4295.

- Rader, C. P., 1996. In *Modern Plastics: Encyclopedia*; McGraw-Hill Co. New York.
- Sirisinha, C., P. Saeoui, and J. Guaysomboon. 2004. "Oil and thermal aging resistance in compatibilized and thermally stabilized chlorinated polyethylene/natural rubber blends." *Polymer* 45:4909–4916.
- Thomassin, J. M et al. 2006. "Improvement of the barrier properties of Nafion® by fluoro-modified montmorillonite." *Solid state ionics* 177:1137–1144.
- Weidisch, R. et al. 2001. "Tetrafunctional multigraft copolymers as novel thermoplastic elastomers." *Macromolecules* 34:6333–6337.
- Wurm, A., M. Ismail, B. Kretschmar, D. Pospiech, and C. Schick. 2010. "Retarded Crystallization in Polyamide/Layered Silicates Nanocomposites caused by an Immobilized Interphase." *Macromolecules* 1–810.
- Yang, I. K, and P. H Tsai. 2007. "Preparation and characterization of polyether-block-amide copolymer/clay nanocomposites." *Polymer Engineering and Science* 47:235–243.
- Zhang, J., L. Jiang, L. Zhu, J. Jane, and P. Mungara. 2006. "Morphology and properties of soy protein and polylactide blends." *Biomacromolecules* 7:1551–1561.
- Zhu, Y. et al. 2006. "Morphology and tensile properties of multigraft copolymers with regularly spaced tri-, tetra-, and hexafunctional junction points." *Macromolecules* 39:4428–4436.

CHAPTER 4

CONCLUSIONS AND FUTURE WORK

4.1 Conclusions

In this thesis, we have systematically studied the two types of composite materials based on fluorinated polymers—fluoroelastomer nanocomposites and fluorothermoplastic elastomer nanocomposites. Peroxide was used as the curing agent for vulcanizing elastomer during the process and methods of treating reinforced nanofillers were introduced. Polymer composites were mixed through Haake torque rheometer and TPE blends containing different reinforced nanofillers were processed by dynamic vulcanization.

In order to better understand the influence of nanofillers on properties of these fluoropolymer nanocomposites, characterization and tests of tensile, DMA, DSC, TGA, SEM, and TEM et al. were performed on these samples. Results of vulcanization kinetics conducted by DSC demonstrated that nanofillers obviously had effects on the cure process of FC2260 nanocomposites. For instance, 4% treated silica in FC2260 significantly increased the cure rate because the activation energy of curing is reduced to 39.2 kJ/mol. This result was in agreement with the conclusions obtained from the mixing analysis by torque rheometry. Mechanical, thermal and thermal dynamic mechanical properties of the nanocomposites displayed clear enhancements compared to that of the neat FC2260. Meanwhile, treated graphite was convinced to prevent the crosslinking process of FC2260 by having higher activation energy than the curing of neat elastomer, and thus failed to introduce reinforcement on FC2260 nanocomposites.

On the other hand, addition of different types of nanofillers to the F-PTE resulted in remarkably different properties. All the used nanofillers could increase tensile properties (e.g. strength, modulus, and elongation), storage modulus, and glass transition temperature of the F-PTE. Like its effect on FKM composites, T-SiO₂ still caused the highest increase in the glass transition temperature and degradation temperature of the elastomer phase in the F-PTE.

However, in contrast to its effect in elastomer nanocomposite, the treated graphite showed a different reinforcing effect on F-TPE. It resulted in the highest tensile properties of the F-PTE. This could be due to T-G's stronger reinforcing effect than T-SiO₂ on the thermoplastic phase of the F-PTE. This could be due to T-G's stronger reinforcing effect than T-SiO₂ on the thermoplastic phase of the F-PTE and good dispersion of the fillers.

The results from this study also suggest that dynamic vulcanization is potentially viable process for the preparation of fluorothermoplastic elastomer.

4.2 Future Work

The investigations in this thesis were mainly focused on the comparison of the effects of several nanofillers on curing behaviors of fluoroelastomer and its dynamically vulcanized thermoplastic elastomer and on mechanical and thermal properties of the resulting nanocomposites. There are many questions unanswered in the exploration of fluoroelastomer and fluorothermoplastic elastomer nanocomposites. Even on the aspect of the nanofiller used, the treatment of silica and graphite can be improved by more strict control and precise characterization. The T-G's reinforcement mechanism on

fluoroelastomer and F-TPE need more detailed study, which may lead to better performance of these polymer nanocomposites. Furthermore, the ratio of fluorothermoplastic to fluoroelastomer has great impact on the phase structure of the TPE and thus varying the ratio will result in different ultimate properties of the TPE blends. Therefore, in the near future we should conduct the following studies: (1) improving treatment methods of nanofillers; (2) identifying the reinforcement mechanism of the treated graphite; (3) improving the compatibility of TPE blends by varying the concentration of the treated silica and; (4) investigating the effect of the thermoplastic/elastomer ratio on the ultimate properties and applications in TPE systems.

APPENDIX—DATA SHEETS OF FC 2260 AND FEP 6322

FC2260 (fluoroelastomer)

Physical Properties	Metric	English	Comments
Specific Gravity	1.8g/cc	1.8g/cc	
Mooney Viscosity	60.0	60.0	ML1+10@121°C
Mechanical Properties	Metric	English	Comments
Hardness Shore A	76	76	Press Cure 7 mins@177°C, Post cure 24hrs @260°C, ASTM D2240
Tensile Strength at Break	16.17MPa	2345psi	Press Cure 7 mins@177°C, Post cure 24hrs @260°C, ASTM D2240
Elongation at Break	225%	225%	Press Cure 7 mins@177°C, Post cure 24hrs @260°C, ASTM D2240
100% Modulus	0.00514GPa	0.745ksi	Press Cure 7 mins@177°C, Post cure 24hrs @260°C, ASTM D2240
Compression Set	25.0%	25.0%	Press Cure 7 mins@177°C, Post cure 24hrs @260°C, ASTM D2240
Thermal Properties	Metric	English	Comments
Transformation Temperature	-18.0°C	-0.400°F	TR10, ASTM D1329
Component Elements Properties	Metric	English	Comments
Fluorine, F	65.9%	65.9%	

FEP 6322(fluorothermoplastic)

Physical Properties	Metric	English	Comments
Specific Gravity	2.15g/cc	2.15g/cc	ASTM D792
Melt Index of Compound	22.0g/10min	22.0g/10min	ASTM D1238
Mechanical Properties	Metric	English	Comments
Tensile Strength at Break	20.0MPa	2900psi	ASTM D638
Elongation at Break	300%	300%	ASTM D638
Izod Impact, Notched	1.98J/cm	3.70ft-lb/in	40 °C, ASTM D256
Thermal Stability	Metric	English	Comments
Melting Point	255 °C	491 °F	ASTM D4591
Brittleness Temperature	<=-70.0 °C	<=-94.0 °F	
Electrical Properties	Metric	English	Comments
Dielectric Constant	<=2.15	<=2.15	ASTM D150
Dielectric Strength	94.5kV/mm	2400kV/in	ASTM D149
Dissipation Factor	<=0.000300	<=0.000300	ASTM D150